

PDF hosted at the Radboud Repository of the Radboud University Nijmegen

The following full text is a publisher's version.

For additional information about this publication click this link.

<http://hdl.handle.net/2066/184415>

Please be advised that this information was generated on 2018-04-11 and may be subject to change.



A search for resonances decaying into a Higgs boson and a new particle X in the $XH \rightarrow qqbb$ final state with the ATLAS detector

The ATLAS Collaboration ^{*}



ARTICLE INFO

Article history:

Received 21 September 2017
Received in revised form 10 January 2018
Accepted 16 January 2018
Available online 3 February 2018
Editor: M. Doser

ABSTRACT

A search for heavy resonances decaying into a Higgs boson (H) and a new particle (X) is reported, utilizing 36.1 fb^{-1} of proton–proton collision data at $\sqrt{s} = 13 \text{ TeV}$ collected during 2015 and 2016 with the ATLAS detector at the CERN Large Hadron Collider. The particle X is assumed to decay to a pair of light quarks, and the fully hadronic final state $XH \rightarrow q\bar{q}b\bar{b}$ is analysed. The search considers the regime of high XH resonance masses, where the X and H bosons are both highly Lorentz-boosted and are each reconstructed using a single jet with large radius parameter. A two-dimensional phase space of XH mass versus X mass is scanned for evidence of a signal, over a range of XH resonance mass values between 1 TeV and 4 TeV, and for X particles with masses from 50 GeV to 1000 GeV. All search results are consistent with the expectations for the background due to Standard Model processes, and 95% CL upper limits are set, as a function of XH and X masses, on the production cross-section of the $XH \rightarrow q\bar{q}b\bar{b}$ resonance.

© 2018 The Author(s). Published by Elsevier B.V. This is an open access article under the CC BY license (<http://creativecommons.org/licenses/by/4.0/>). Funded by SCOAP³.

1. Introduction

The Standard Model (SM), including the recently discovered Higgs boson [1,2], describes collider phenomenology for energy scales up to a few hundred GeV. However, a number of issues with the SM, including sensitivity of the Higgs boson mass to radiative corrections, indicate either extreme fine-tuning or the presence of new physics at an energy scale not far above the Higgs boson mass. Many theoretical extensions to the SM predict the existence of new particles around the TeV scale, and it is natural to expect such particles to exhibit significant coupling to the Higgs boson (H). Examples of previous studies at the CERN Large Hadron Collider (LHC) which are motivated by these considerations include ATLAS [3,4] and CMS [5–8] searches for new resonances decaying into VH , where V denotes a W or Z boson, as well as ATLAS [9] and CMS [10,11] searches for resonances decaying into HH .

This Letter presents a new and more general search for heavy resonances which decay into the SM Higgs boson and a new particle (X), utilizing a data sample corresponding to 36.1 fb^{-1} of proton–proton (pp) collisions at $\sqrt{s} = 13 \text{ TeV}$ collected during 2015 and 2016 with the ATLAS detector. Since the hypothetical particle X has not yet been detected, it has unknown properties. It is assumed that X decays hadronically into a pair of light quarks, $X \rightarrow q\bar{q}$, and has a natural width which is narrow compared to the detector resolution. It is also assumed that single X produc-

tion is sufficiently rare that it has not been observed by analyses such as the ATLAS and CMS searches for dijet resonances [12–14].

Examples of theories of physics beyond the SM which predict the existence of XH resonances include pseudo Nambu–Goldstone models [15], extended Higgs sectors [16] and extra-dimension frameworks with warped compactifications [17]. For simplicity, such XH resonances are hereafter denoted by Y . It is assumed that the new resonance Y is narrow. This study analyses the decay chain $Y \rightarrow XH \rightarrow q\bar{q}b\bar{b}$, and considers the regime of high Y masses, in the range between 1 TeV and 4 TeV, with $m(Y) \gg m(X)$, which implies that the X and H bosons are both highly Lorentz-boosted. The X and H boson candidates are each reconstructed in a single jet with large radius parameter; these jets are called “large- R jets” throughout this Letter and are denoted by J . Jet substructure techniques and b -tagging are used to suppress the dominant background from multijet events, to enhance the sensitivity to the dominant $H \rightarrow b\bar{b}$ decay mode, and to distinguish between the two bosons.

Given their assumed decay modes, both X and Y must be bosons. However, the search does not impose explicit requirements on their electric charge, spin or polarization states, and utilizes a simple event selection that does not seek to exploit angular correlations or other variables that would be sensitive to particular spin states. The analysis utilizes the reconstructed Y mass as the final discriminant, searching for an excess due to a resonance in the $Y \rightarrow XH \rightarrow JJ$ mass distribution, separately in a large number of overlapping ranges of X mass.

^{*} E-mail address: atlas.publications@cern.ch.

A modified form of the benchmark heavy vector triplet (HVT) model [18,19] is used to provide a measure of the implications of the results of the search within one particular theoretical framework. The HVT model provides a simplified phenomenological Lagrangian that predicts heavy spin-1 resonances which are produced via $q\bar{q}$ annihilation, and which can have significant branching ratios for decays into boson pairs, with longitudinally polarized bosons. The search results are used to set limits on the production cross-section $\sigma(pp \rightarrow Y \rightarrow XH \rightarrow q\bar{q}'b\bar{b})$ within the HVT theoretical framework, to provide an interpretation in the case where both X and Y have spin 1. The search overlaps with the VH and HH searches, when the X mass window extends around the V and H mass values, respectively, in which cases the results are found to be compatible with those analyses. However, the current search considers a much wider range of X masses, from 50 GeV to 1000 GeV.

2. ATLAS detector

The ATLAS detector [20] is a general-purpose particle physics detector used to investigate a broad range of physics processes. ATLAS includes an inner detector (ID) surrounded by a superconducting solenoid, electromagnetic (EM) and hadronic calorimeters, and a muon spectrometer (MS). The ID consists of a silicon pixel detector, including the insertable B-layer [21] installed after Run 1 of the LHC, a silicon microstrip detector and a straw-tube tracker. The ID is immersed inside a 2 T axial magnetic field from the solenoid and provides precision tracking of charged particles with pseudorapidity¹ $|\eta| < 2.5$. The straw-tube tracker also provides transition radiation measurements for electron identification. The calorimeter system consists of finely segmented sampling calorimeters using lead/liquid-argon for the detection of EM showers up to $|\eta| = 3.2$, and copper or tungsten/liquid-argon for hadronic showers for $1.5 < |\eta| < 4.9$. In the central region ($|\eta| < 1.7$), a steel/scintillator hadronic calorimeter is used. Outside the calorimeters, the MS incorporates multiple layers of trigger and tracking chambers within a magnetic field produced by a system of superconducting toroids, enabling an independent precise measurement of muon track momenta for $|\eta| < 2.7$. The ATLAS detector has a two-level trigger system. The first-level (L1) trigger is implemented in hardware and uses the calorimeter and muon systems to reduce the accepted event rate to 100 kHz. The L1 trigger is followed by a software-based high-level trigger to reduce the accepted event rate to approximately 1 kHz for offline analysis [22].

3. Signal and background simulation

Samples of simulated signal and background events are used to optimize the event selection and to estimate the background contributions from various SM processes.

The $Y \rightarrow XH$ signal was simulated by modifying the HVT [18, 19] configuration for $W' \rightarrow WH$ decays, replacing the W' boson with a narrow resonance Y , and the W boson by X . The new X boson was assumed to have spin 1, a natural width of 2 GeV, and a branching ratio (B) of 100% for decays $X \rightarrow u\bar{d}$. The properties of the Higgs boson were assumed to be as described in the SM, with its mass set to 125.5 GeV and decays into $b\bar{b}$ and $c\bar{c}$ enabled

in the simulation. Given the SM branching ratios and the relevant experimental performance factors, Higgs boson decays to $b\bar{b}$ dominate the signal efficiency. The signal samples were generated with MADGRAPH5_aMC@NLO 2.2.2 [23] interfaced to PYTHIA 8.186 [24] for parton shower and hadronization, with the NNPDF2.3 next-to-leading-order (NLO) parton distribution function (PDF) set [25] and the ATLAS A14 set of tuned parameters (tune) [26] for the underlying event. Approximately 100 signal samples were generated, each with individual values of Y and X masses, chosen in a two-dimensional grid of values ranging from 1 TeV to 4 TeV for $m(Y)$ and from 50 GeV to 1000 GeV for $m(X)$. The requirements $m(Y) > 1$ TeV and $m(Y) \gg m(X)$ were applied, to focus on the kinematic regime where the X and H bosons are highly Lorentz-boosted.

The dominant SM background is due to multijet processes and, as described in Section 7, is evaluated using data-driven techniques. Some cross-checks were performed using simulated multijet events generated with PYTHIA 8.186, with the NNPDF2.3 NLO PDF and the ATLAS A14 tune.

Minor background contributions, which are estimated using simulated samples, are due to $t\bar{t}$ production and to vector boson production in association with jets (V +jets). The $t\bar{t}$ samples were generated with POWHEG-Box v2 [27] with the CT10 PDF set [28], interfaced with PYTHIA 6.428 [29] and the Perugia 2012 tune for the parton shower [30] using the CTEQ6L1 PDF set [31]. The cross-section of the $t\bar{t}$ process was normalized to the result of a QCD calculation at next-to-next-leading order and next-to-next-leading logarithmic accuracy (NNLO+NNLL), as implemented in TOP++ 2.0 [32]. The V +jets background samples were generated with SHERPA 2.1.1 [33] interfaced with the CT10 PDF set, including only hadronic V decays. Matrix elements of up to four extra partons were calculated at leading order in QCD. The V +jets events are normalized to the NNLO cross-sections [34].

For all simulated samples except those produced using SHERPA, EVTGEN v1.2.0 [35] was used to model the properties of bottom and charm hadron decays. The effect of multiple pp interactions in the same and neighbouring bunch crossings (pile-up) was included by overlaying minimum-bias events simulated with PYTHIA 8.186 on each generated event [36]. The detector response was simulated with a GEANT4 [37] based framework [38] and the events were processed with the same reconstruction software as that used for data.

4. Event reconstruction

The reconstruction and identification of hadronically decaying bosons is performed using jets. Large- R jets are reconstructed with the anti- k_t algorithm [39,40] with radius parameter $R = 1.0$ from three-dimensional topological clusters of energy deposits in the calorimeter [41]. The large- R jets are required to have transverse momentum $p_T > 250$ GeV and $|\eta| < 2.0$.

Track-jets are formed from charged-particle tracks with $p_T > 0.4$ GeV and $|\eta| < 2.5$ that satisfy a set of hit and impact parameter criteria to reduce the contamination from pile-up interactions, and are clustered using the anti- k_t algorithm with $R = 0.2$ [42]. Only track-jets with $p_T > 25$ GeV that are constructed from at least two tracks are considered in this analysis.

To mitigate pile-up effects and soft radiation, the large- R jets are trimmed [43], and then are subsequently reclustered into subjets using the k_t algorithm [44]. To compensate for the limited angular resolution of the calorimeter, the mass of large- R jets is computed using a combination of calorimeter and tracking information [45]. The combined jet mass is defined as

¹ ATLAS uses a right-handed coordinate system with its origin at the nominal interaction point (IP) in the centre of the detector and the z -axis along the beam pipe. The x -axis points from the IP to the centre of the LHC ring, and the y -axis points upwards. Cylindrical coordinates (r, ϕ) are used in the transverse plane, ϕ being the azimuthal angle around the beam pipe. The pseudorapidity is defined in terms of the polar angle θ as $\eta = -\ln \tan(\theta/2)$. Angular distance is measured in units of $\Delta R \equiv \sqrt{(\Delta\eta)^2 + (\Delta\phi)^2}$.

$$m_J \equiv w_{\text{calo}} \times m_J^{\text{calo}} + w_{\text{track}} \times \left(m_J^{\text{track}} \frac{p_T^{\text{calo}}}{p_T^{\text{track}}} \right),$$

where m_J^{calo} is the calorimeter-only estimate of the jet mass. The variable m_J^{track} is the jet mass estimated via tracks with $p_T > 0.4$ GeV associated with the large- R jet using “ghost association” [39], and is scaled in the combined mass formula by the ratio of calorimeter to track p_T estimates in order to account for the missing neutral-particle component in the track-jet. The ghost association technique relies on repeating the jet clustering process with the addition of measured tracks that have the same direction but infinitesimally small p_T , so that the jet properties remain unaffected. A track is associated with a jet if it is contained in the jet after this re-clustering procedure. The weighting factors w_{calo} and w_{track} depend on p_T satisfy $w_{\text{calo}} + w_{\text{track}} = 1$, and are used to optimize the combined mass resolution. To partially account for the energy carried by muons from semileptonic b -hadron decays, the four-momentum of the closest muon candidate satisfying “Tight” muon identification criteria [46] with $p_T > 4$ GeV and $|\eta| < 2.5$ that is within $\Delta R = 0.2$ of a track-jet that is b -tagged is added to the calorimeter jet four-momentum [47]. In this study, only large- R jets with $m_J > 50$ GeV are considered for further analysis.

Identifying a large- R jet as a hadronically decaying Higgs boson candidate is aided by using track-jets matched via ghost association to the large- R jet [48]. The identification of b -hadrons relies on a multivariate b -tagging algorithm [49] applied to a set of tracks in a region of interest around each track-jet axis. The b -tagging requirements result in an efficiency of 77% for track-jets containing b -hadrons, and the misidentification rate is $\sim 2\%$ ($\sim 24\%$) for light-flavour (charm) jets. These were determined in a sample of simulated $t\bar{t}$ events. For simulated samples the b -tagging efficiencies are corrected, based on the jet p_T , to match those measured in data [50].

Identifying a large- R jet as a hadronically decaying $X \rightarrow q\bar{q}'$ boson candidate is aided by using jet substructure techniques. The variable D_2 is defined² as a ratio of two- and three-point energy correlation functions [51,52], which are based on the energies and pairwise angular distances of particles within a jet. This variable is optimized [53] to distinguish between jets originating from a single parton and those from the two-body decay of a heavy particle. A detailed description of the optimization, performed using simulated V decays, can be found in Refs. [54,55]. Studies of boosted W boson decays [54] demonstrate that the D_2 variable is well modelled, with good agreement observed between data and simulation.

“Loose” electrons and muons are reconstructed and identified as described in Refs. [46,56]. These leptons have $p_T > 7$ GeV, $|\eta| < 2.5$ (2.47) for muons (electrons), $|d_0|/\sigma_{d_0} < 3$ (5) and $|z_0 \sin \theta| < 0.5$ mm, where d_0 is transverse impact parameter with respect to the beam line, σ_{d_0} is the corresponding uncertainty, and z_0 is the distance between the longitudinal position of the track along the beam line at the point where d_0 is measured and the longitudinal position of the primary vertex. An isolation criterion is also applied. Specifically, within a cone of size $\Delta R = 0.2$ (0.3) around an electron (muon), the scalar sum of transverse momenta of tracks divided by the lepton p_T is required to be less than a cut-off value, chosen to provide a constant efficiency of around 99% as a function of p_T and $|\eta|$.

5. Event selection

Events are selected from the 2015 (2016) running period using a trigger that requires a single large- R jet with $p_T >$

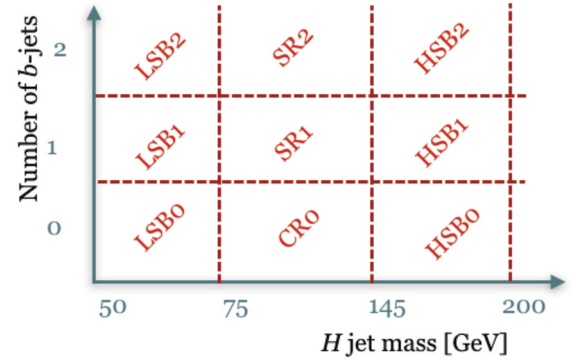


Fig. 1. Illustration of the definitions of the various mutually exclusive data regions. The data are divided into Low Sidebands (LSB), Signal Regions (SR), and High Sidebands (HSB) according to the mass of the candidate Higgs jet. Each region is subdivided further according to the number of b -tagged jets associated with the candidate Higgs jet. The 0-tag sample satisfying the SR mass cut is denoted by CR0 to emphasize its use as a control region in the background determination, rather than as an additional signal region.

360 (420) GeV. Selected events are required to have at least one primary vertex (PV) that has at least two associated tracks, each with transverse momentum $p_T > 0.4$ GeV. For events with more than one PV candidate, the one with the largest track $\sum p_T^2$ is chosen as the hard-scatter PV. To select a hadronic final state, events with one or more “Loose” charged leptons (electrons or muons) are vetoed.

Events are kept only if they contain at least two large- R jets. For events with more than two large- R jets, only the two “leading” jets, namely those with highest p_T , are considered as possible X and H candidates. To ensure high and uniform trigger efficiency, the leading large- R jet must satisfy $p_T > 450$ GeV.

Additional requirements are imposed to distinguish hadronically decaying boson candidates from background jets. To be identified as a Higgs jet candidate, the combined mass of the jet is required to satisfy $75 \text{ GeV} < m_J < 145 \text{ GeV}$, a criterion that is $\sim 90\%$ efficient for Higgs boson jets. The number of b -tagged jets inside the Higgs jet is used to categorize the events in two orthogonal signal regions: the “1-tag” signal region (SR1) and “2-tag” signal region (SR2) definitions require Higgs candidates to contain exactly one and two b -tagged jets, respectively. The SR1 region recovers some efficiency loss in the high Y mass region where the angular separation between the two b -quarks from the Higgs decay is small and the fragmentation products are merged [47]. As depicted in Fig. 1 and described in Section 7, a number of different samples of events are selected to be used as part of the background estimation strategy. These samples include events with the Higgs jet candidate with a mass in the so-called “high sideband” (HSB) region with $145 \text{ GeV} < m_J < 200 \text{ GeV}$, as well as events in a “low sideband” (LSB) region with $50 \text{ GeV} < m_J < 75 \text{ GeV}$. In addition, “0-tag” samples, with Higgs candidates that pass these various mass requirements but have no associated b -tagged jets, are also selected. The 0-tag sideband samples are denoted by LSB0 and HSB0. The 0-tag sample satisfying the SR mass cut is denoted by CR0 to emphasize its use as a control region in the background determination (see Section 7), rather than as an additional signal region.

If both large- R jets fulfil the Higgs mass requirement, the jet with the highest number of associated b -tagged jets is chosen as the Higgs candidate. In case both have the same number of b -tagged jets, the ambiguity is resolved by assigning the leading p_T large- R jet as the Higgs candidate. Studies of signal samples with $m(X) = 110$ GeV demonstrate that, in the lower $m(Y)$ region, the probability to correctly identify the H and X jets is 98.8%. This

² The angular exponent β , defined in Ref. [51], is set to unity.

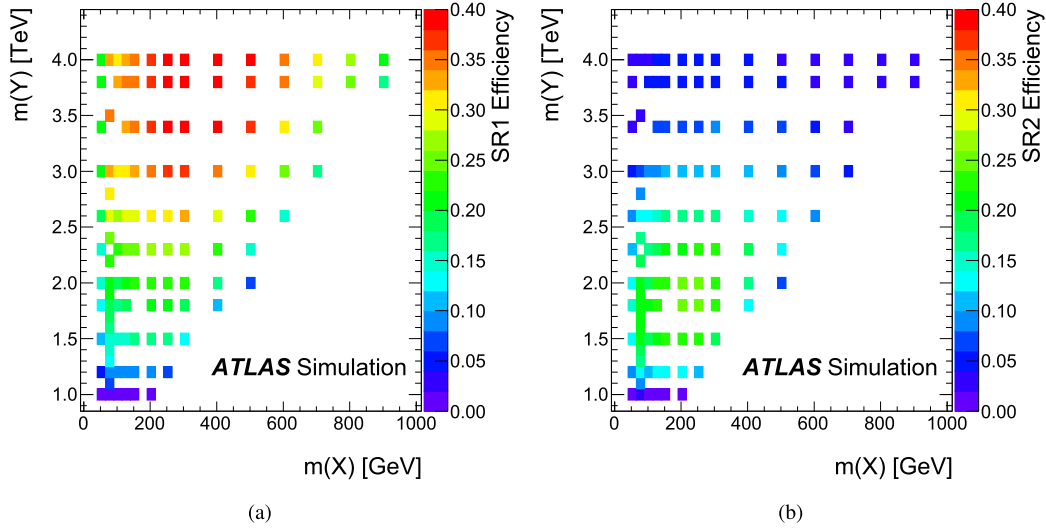


Fig. 2. Efficiencies, as a function of $m(Y)$ and $m(X)$ for all the generated signal samples, for the selection defining (a) the 1-tag signal region (SR1) and (b) the 2-tag signal region (SR2). (For interpretation of the references to colour in this figure, the reader is referred to the web version of this article.)

value decreases to 89.5% for $m(Y) = 4$ TeV, due to the falling efficiency in the very high mass region to tag two separate b -tagged jets within the H jet.

The large- R jet which is not chosen as the Higgs candidate is assigned to the X hypothesis. The jet substructure variable D_2 , described previously, is used to check whether the X candidate jet is compatible with the two-prong structure expected due to its assumed $X \rightarrow q\bar{q}'$ decay. The requirement on the value of D_2 corresponds to that defined in Refs. [54,55] to provide a constant efficiency of 50% for selecting hadronic V decays, when applied along with an associated requirement that m_J lies within a window around the V mass. Given that the X mass is a priori unknown, the event selection does not make any requirement on the mass of the X candidate jet beyond the $m_J > 50$ GeV restriction applied to all large- R jets, however the data are interpreted in windows of m_X .

The mass of the $Y \rightarrow XH$ candidate is required to be larger than 1 TeV. The efficiencies for the 1-tag and 2-tag signal region selections are presented as a function of $m(Y)$ and $m(X)$ in Fig. 2 for the various signal samples. No signal samples with $m(Y) > 4$ TeV were simulated, due to the low expected sensitivity for such high masses with the current data sample. However, data events with higher reconstructed Y mass values are included in the overflow bin in the mass distributions.

6. Signal modelling

The signal search in the two-dimensional space of $m(Y)$ versus $m(X)$ employs a sliding-window technique to the m_J spectrum of the X candidate jet, dividing the data into a series of overlapping m_J ranges. As described in Section 9, for each m_J window of the X candidate jet, the corresponding m_{JJ} distribution is examined for evidence of an excess due to a signal, where m_{JJ} denotes the invariant mass of the system formed by the H and X candidate large- R jets.

The reconstructed X mass resolution varies from 12 GeV to 40 GeV. The widths of the overlapping m_J windows for the X candidate jet are chosen to be around twice the X mass resolution, but also take into account the limited number of data events. The central values of neighbouring m_J windows are shifted by roughly half of the X mass resolution, ensuring that they overlap and do not leave gaps in the search coverage. Studies in which simulated

signals were injected at various mass values were used to demonstrate the reasonableness of the window choices.

The reconstructed $Y \rightarrow XH$ mass resolution varies from about 65 GeV to 100 GeV. For each m_J window of the X candidate jet, the binning for the corresponding m_{JJ} distribution is chosen to be at least as large as the Y mass resolution, dependent on the size of the data sample.

Given the large number of possible $m(Y)$ and $m(X)$ values in the ranges considered, a parameterization of the signal is used to interpolate between the mass values for which signal samples were generated. Probability distribution functions for the m_{JJ} and m_J shapes are built using the RooKeysPdf class of the RooFit package [57]. Multidimensional morphing methods, implemented in the RooMomentMorphND class [58], are subsequently applied to parameterize grid points using the surrounding four nearby points. The normalization of the parameterized signals is estimated using linear interpolation.

7. Background estimation

After the event selection, over 96% of the SM background originates from multijet processes. A data-driven method is used to determine the shape of the dominant multijet background, with its normalization in the signal regions being determined with the fit procedure described in Section 9. The small additional background contributions from $t\bar{t}$ and V +jets production are estimated via simulation. The background determination is performed separately in each of the m_J windows considered for the X candidate jet mass.

As depicted in Fig. 1, the event sample, before any specific requirements are made on the mass of the X candidate jet, is separated into mutually exclusive categories according to the mass and number of b -tagged jets of the Higgs boson candidate. The SR1 and SR2 regions are used to perform the signal search, while the other seven regions are used as control regions to develop and validate the background model. The multijet background component in each of the seven control regions is determined by subtracting from the data the $t\bar{t}$ and V +jets contributions predicted by simulation.

The modelling of the dominant multijet background in the SR1 and SR2 signal regions starts from the CR0 sample, for which the candidate Higgs jet satisfies the SR requirement on the jet mass but has no associated b -tagged jets. The CR0 sample should contain negligible signal contamination. The basic strategy is to use

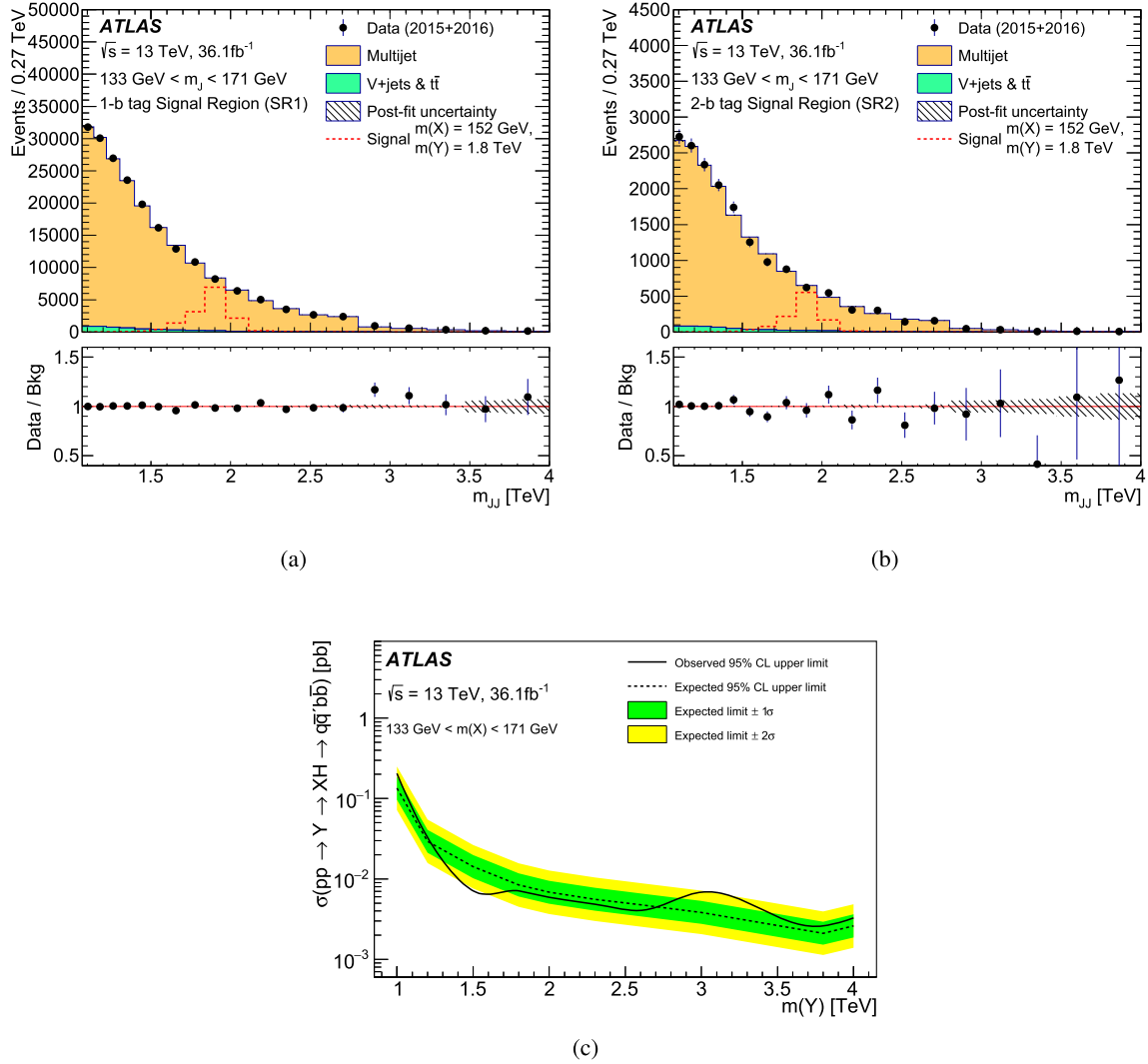


Fig. 3. The m_{JJ} mass distributions in the m_J window of the X candidate jet from 133 GeV to 171 GeV after the likelihood fit for events in (a) the 1-tag signal region (SR1) and (b) the 2-tag signal region (SR2). The highest mass bin includes any overflows. The background expectation is given by the filled histograms and the ratio of the observed data to the background (Data/Bkg) is shown in the lower panel. The uncertainties shown are those after the fit described in the text. One particular example of a possible signal model, namely with $m(X) = 152$ GeV and $m(Y) = 1.8$ TeV, is overlaid with an arbitrary overall normalization, illustrating the corresponding contributions that would be expected in the SR1 and SR2 regions. Panel (c) shows the resultant 95% CL upper limit on the production cross-section, $\sigma(pp \rightarrow Y \rightarrow XH \rightarrow q\bar{q}b\bar{b})$. (For interpretation of the references to colour in this figure, the reader is referred to the web version of this article.)

events in the CR0 sample with at least one (two) track-jet(s) associated with the Higgs jet to model the shape of the multijet background in the SR1 (SR2) signal region. However, sources of possible differences between the multijet components of CR0 versus SR1 and SR2 include changes in the underlying event populations due to the absence or presence of b -quarks as well as kinematic differences arising from the application of b -tagging, since the b -tagging efficiency depends on the p_T and η of the track-jet. The corrections required to take these differences into account are extracted from the HSB events. In each of the HSB regions with different number of b -tags (HSB0, HSB1, HSB2), a pair of two-dimensional histograms is filled, one of p_T versus η for the leading track-jet, and the other for the subleading track-jet. Subsequently, leading and subleading track jet reweighting maps are created by dividing the HSB1 and HSB2 histograms by the corresponding HSB0 histogram. A Gaussian kernel, similar to that applied in Ref. [59], is used to smooth out statistical fluctuations by taking a weighted sum of neighbouring bins. The weight is inversely proportional to the width of the Gaussian kernel and depends on the statistical

uncertainty of each bin. The result is a reduction of statistical fluctuations, while adding negligible bias to the distributions.

To describe the SR multijet background shapes, the CR0 events are reweighted using the maps in bins of track-jet p_T and η extracted from the sideband. The reweighting is performed only for the 2-tag samples, as the modelling of the shape of the multijet background in the 1-tag sideband regions without reweighting is observed to be adequate. Due to the correlations between the kinematic variables of the two leading track-jets used for the reweighting, multiple reweighting iterations are performed, until the track-jet properties, p_T and η , are matched within statistical uncertainties.

The background modelling is validated by using the same method to predict the background in the LSB regions in the low mass sidebands, and then comparing with the data and obtaining good agreement. Agreement is also confirmed in the signal region by integrating over all values of the mass of the X candidate jet, thereby diluting any possible signal contamination to a negligible level.

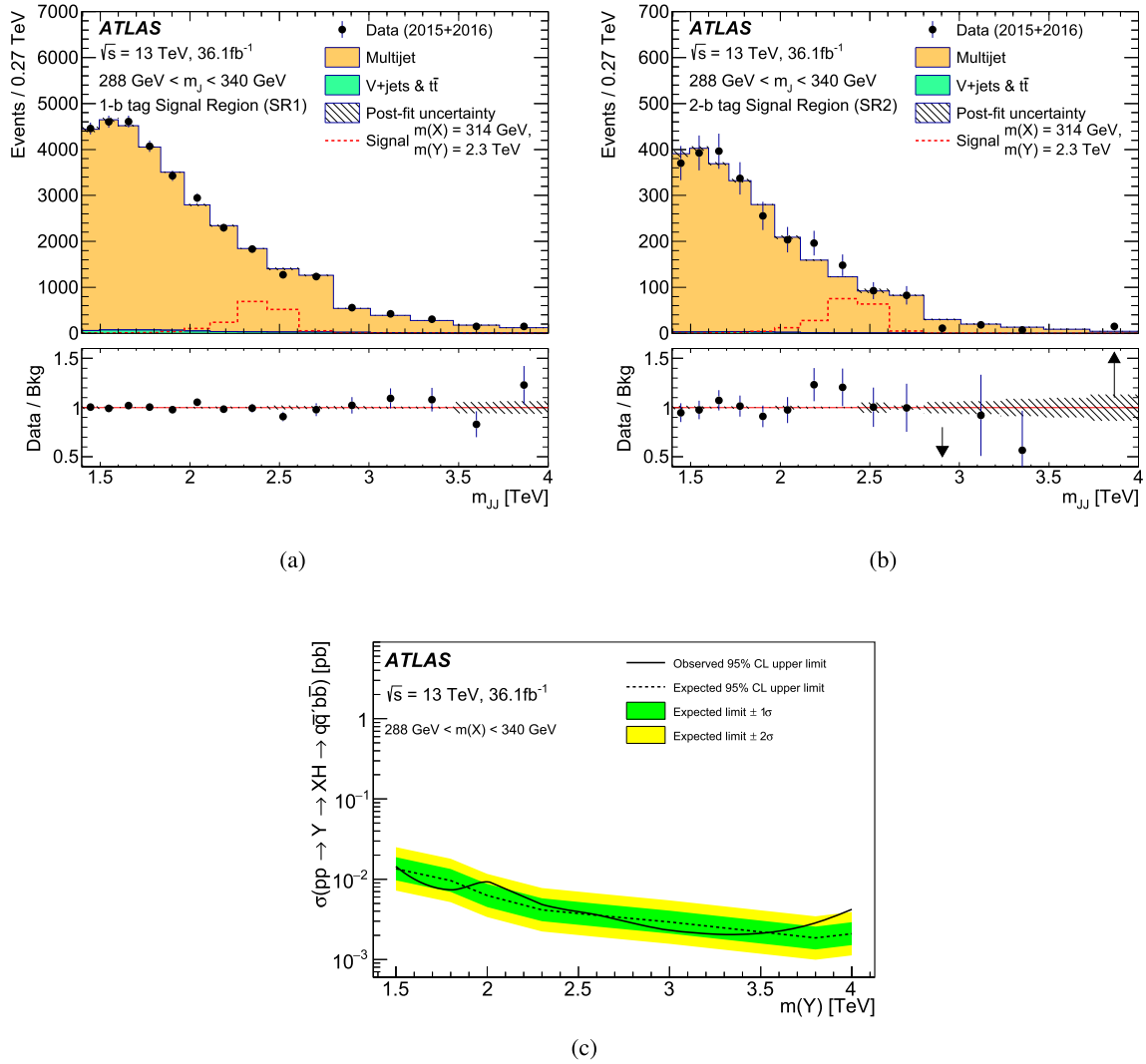


Fig. 4. The m_{JJ} mass distributions in the m_J window of the X candidate jet from 288 GeV to 340 GeV after the likelihood fit for events in (a) the 1-tag signal region (SR1) and (b) the 2-tag signal region (SR2). The highest mass bin includes any overflows. The background expectation is given by the filled histograms and the ratio of the observed data to the background (Data/Bkg) is shown in the lower panel. The uncertainties shown are those after the fit described in the text. One particular example of a possible signal model, namely with $m(X) = 314$ GeV and $m(Y) = 2.3$ TeV, is overlaid with an arbitrary overall normalization, illustrating the corresponding contributions that would be expected in the SR1 and SR2 regions. Panel (c) shows the resultant 95% CL upper limit on the production cross-section, $\sigma(pp \rightarrow Y \rightarrow XH \rightarrow q\bar{q}b\bar{b})$. (For interpretation of the references to colour in this figure, the reader is referred to the web version of this article.)

8. Systematic uncertainties

The main systematic uncertainty in the background estimate arises from the potential mis-modelling of the background processes. As described in Section 7, the multijet background shapes in the two signal regions are estimated directly from data using sideband regions. To determine the systematic uncertainty in this method, the multijet background shapes in the HSB1 and HSB2 regions are compared, in each m_J window of the X candidate jet, to those of the reweighted HSB0 multijet distributions. The differences, in bins of m_{JJ} , fitted with a line are used as the multijet modelling systematic uncertainties. The largest observed shape difference is found to be approximately 12%, while the smallest is 3%. A normalization uncertainty of 30% is assigned to the small $t\bar{t}$ background, based on the ATLAS $t\bar{t}$ differential cross-section measurement [60]. The same uncertainty is conservatively applied to the small V +jets background component.

The uncertainty in the combined 2015+2016 integrated luminosity is 2.1%. It is derived, following a methodology similar to that detailed in Ref. [61], from a calibration of the luminosity scale

using x - y beam-separation scans performed in August 2015 and May 2016. This uncertainty is applied to the yields of both the signal and the small $t\bar{t}$ and V +jets backgrounds, which are not determined from data.

Additional systematic uncertainties in the signal acceptance arise from the choice of PDF set and the uncertainty in the amount of initial- and final-state radiation. For all the two-dimensional mass grid points, a constant 5% uncertainty is applied and covers both effects.

Uncertainties related to the signal parameterization method are estimated by comparing the mass distributions of generated signal points to those predicted from morphing nearby points in the two-dimensional space of $m(Y)$ versus $m(X)$. The largest observed normalization deviation is $\sim 8\%$, while differences in the signal shape also reach levels up to $\sim 8\%$. Both effects are included as uniform uncorrelated systematic uncertainties.

Systematic uncertainties which account for experimental effects on the signal shape include the large- R jet mass scale and mass resolution, as well as D_2 and the b -tagging. The impact of each of these effects is evaluated by shifting each variable accord-

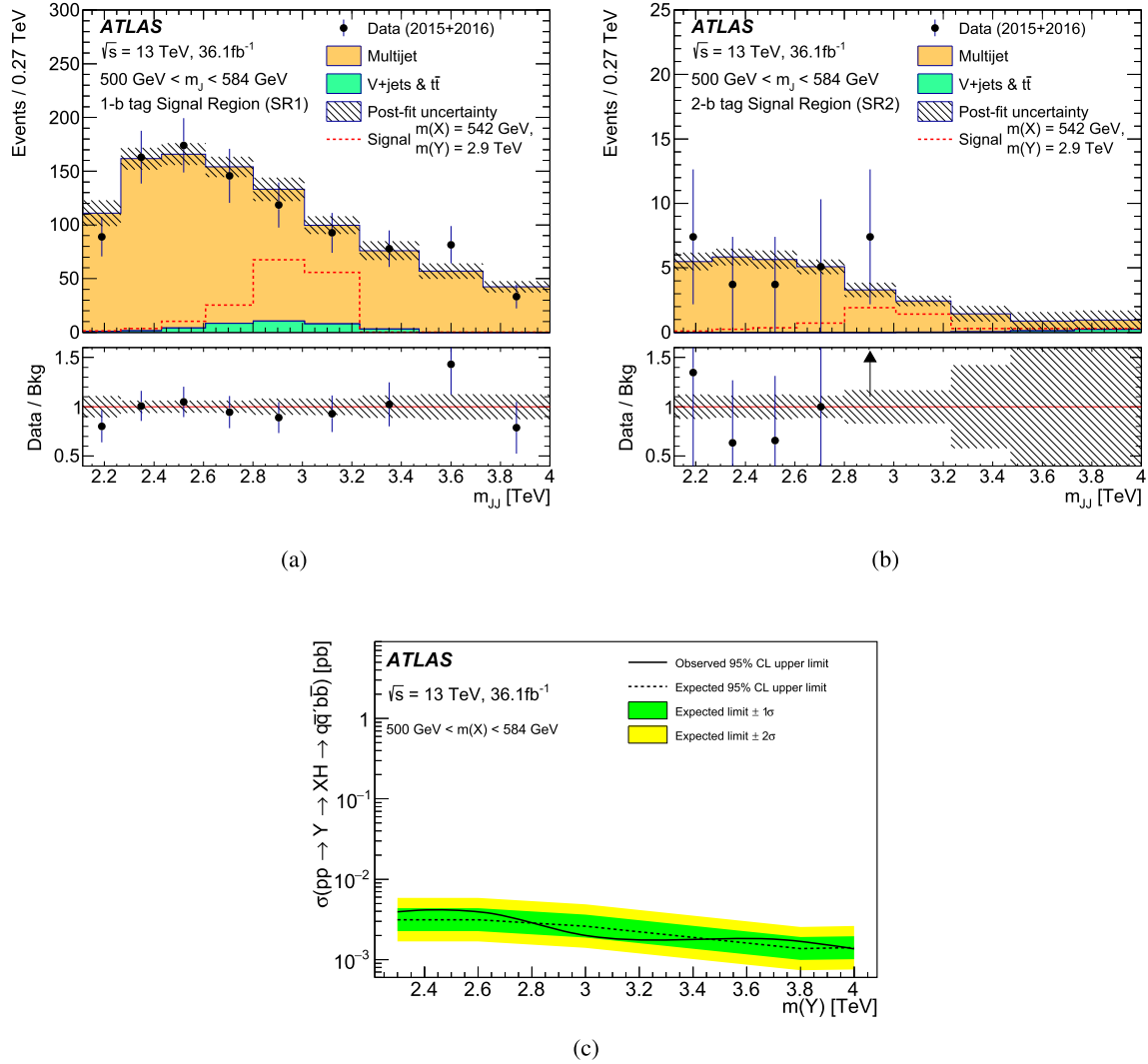


Fig. 5. The m_{JJ} mass distributions in the m_J window of the X candidate jet from 500 GeV to 584 GeV after the likelihood fit for events in (a) the 1-tag signal region (SR1) and (b) the 2-tag signal region (SR2). The highest mass bin includes any overflows. The background expectation is given by the filled histograms and the ratio of the observed data to the background (Data/Bkg) is shown in the lower panel. The uncertainties shown are those after the fit described in the text. One particular example of a possible signal model, namely with $m(X) = 542$ GeV and $m(Y) = 2.9$ TeV, is overlaid with an arbitrary overall normalization, illustrating the corresponding contributions that would be expected in the SR1 and SR2 regions. Panel (c) shows the resultant 95% CL upper limit on the production cross-section, $\sigma(pp \rightarrow Y \rightarrow XH \rightarrow q\bar{q}b\bar{b})$. (For interpretation of the references to colour in this figure, the reader is referred to the web version of this article.)

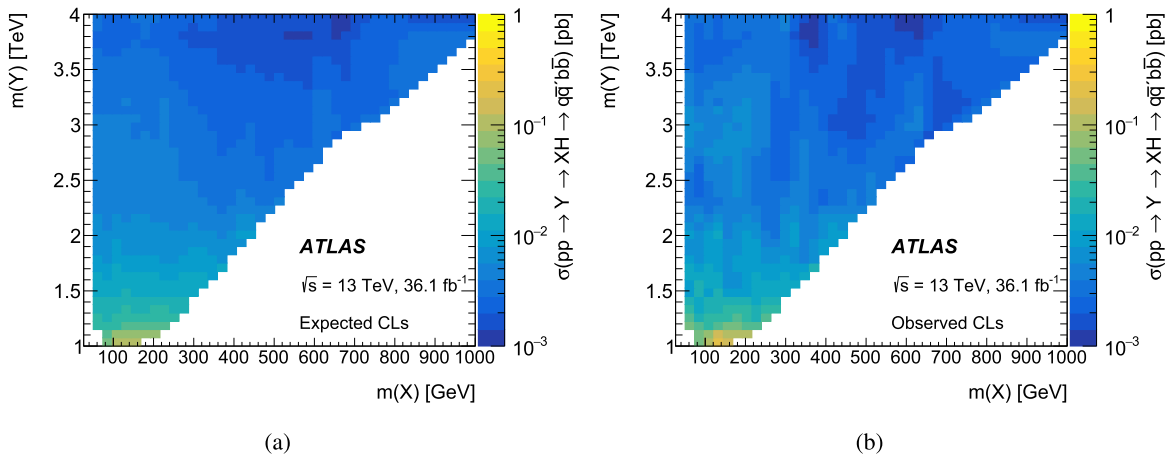


Fig. 6. The (a) expected and (b) observed 95% CL limits on the production cross-section $\sigma(pp \rightarrow Y \rightarrow XH \rightarrow q\bar{q}b\bar{b})$ (z-axis) in the two-dimensional space of $m(Y)$ versus $m(X)$. (For interpretation of the references to colour in this figure, the reader is referred to the web version of this article.)

ing to these systematic uncertainties and then re-performing the signal parameterization. Based on the measurements documented in Refs. [55,62], a 2% uncertainty is assigned for the large- R jets p_{T} scale, while uncertainties of 20% and 15%, respectively, are assigned for the large- R jet mass resolution and D_2 resolution. Uncertainties in the correction factors for the b -tagging are applied to the simulated event samples by looking at dedicated flavour-enriched samples in data. An additional term is included to extrapolate the measured uncertainties to the high- p_{T} region of interest. This term is calculated from simulated events by considering variations of the quantities affecting the b -tagging performance such as the impact parameter resolution, percentage of poorly measured tracks, description of the detector material, and track multiplicity per jet. The dominant effect on the uncertainty when extrapolating to high p_{T} is related to the change in tagging efficiency when smearing the track impact parameters based on the resolution measured in data and simulation. The uncertainty in the b -tagging efficiency is measured as a function of b -jet p_{T} and η for track-jets with $p_{\text{T}} < 250$ GeV, while for higher p_{T} values it is extrapolated using simulation [50]. These uncertainties vary between 2% and 8% in the lower p_{T} range, and rise to approximately 9% for track-jets with $p_{\text{T}} > 400$ GeV.

9. Statistical treatment and results

The signal search in the two-dimensional space of $m(Y)$ versus $m(X)$ is performed by applying a sliding-window technique to the m_j spectrum of the X candidate jet, which divides the data into a series of overlapping m_j ranges. For each m_j window, a binned maximum-likelihood fit is then performed to the resultant m_{jj} distributions in both SR1 and SR2 signal regions simultaneously. A test statistic based on the profile likelihood ratio [63] is used to test hypothesized values of the global signal strength (μ), corresponding to the HVT model. The systematic uncertainties, described previously, are modelled with Gaussian or log-normal constraint terms (nuisance parameters) in the definition of the likelihood function.

Each m_j window of the X candidate jet is fitted independently, but as the mass ranges overlap, the fit results are correlated. In each fit, the normalizations of the multijet backgrounds in the SR1 and SR2 signal regions are treated as free parameters. All of the systematic uncertainties are treated as correlated between the two signal regions.

The data distributions and fit results are shown for three example m_j windows of the X candidate jet in Figs. 3–5. In each case, the left (right) upper plot shows the m_{jj} distribution in the SR1 (SR2) signal region, and the results of the simultaneous fit are superimposed on the plots. Examples of possible signal models are also shown, with arbitrary overall normalization, illustrating the corresponding contributions that would be expected in the SR1 and SR2 regions. The data distributions are well described by the fitted SM background, and there is no significant evidence of a signal. The same conclusion is valid for all m_j windows of the X candidate jet.

The fits to the data are used to set upper limits on the production cross-section, $\sigma(pp \rightarrow Y \rightarrow XH \rightarrow q\bar{q}b\bar{b})$. Exclusion limits are computed using the CL_s method [64], with a value of μ regarded as excluded at the 95% confidence level (CL) when CL_s is less than 5%. The corresponding limit plots are included in panel (c) of Figs. 3–5.

A summary of the expected and observed 95% CL limits on the production cross-section, $\sigma(pp \rightarrow Y \rightarrow XH \rightarrow q\bar{q}b\bar{b})$, is given in the two-dimensional plane of $m(Y)$ versus $m(X)$ in Fig. 6. For X mass windows around the V and Higgs boson mass values, the results are found to be compatible with the dedicated ATLAS VH

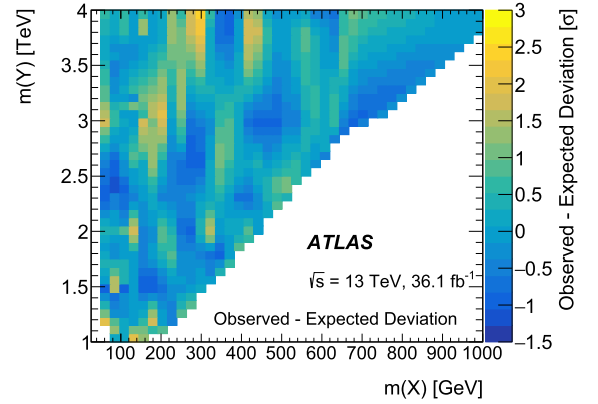


Fig. 7. Differences between the observed and the expected 95% CL limits on the resonance production cross-section $\sigma(pp \rightarrow Y \rightarrow XH \rightarrow q\bar{q}b\bar{b})$, expressed in terms of multiples of σ , the equivalent Gaussian significance. (For interpretation of the references to colour in this figure, the reader is referred to the web version of this article.)

and HH searches reported in Refs. [4] and [9], respectively. To visualize both the magnitude and the sign of discrepancies between the expected and observed limits, Fig. 7 presents the differences between the expected and observed limits, expressed in multiples of σ , the equivalent Gaussian significance. The maximum observed deviation has a local significance of about 2.5σ , corresponding to a global deviation of 1.2σ .

10. Conclusion

A search for new heavy resonances Y decaying into a Higgs boson and a new particle X was carried out using 36.1 fb^{-1} of pp collision data collected at $\sqrt{s} = 13 \text{ TeV}$ by ATLAS during the 2015 and 2016 runs of the CERN Large Hadron Collider. The $Y \rightarrow XH \rightarrow q\bar{q}b\bar{b}$ channel was studied using a generic approach in the topological regime where both bosons are highly Lorentz-boosted, and each is reconstructed as a single jet with a large radius parameter. Jet substructure and b -tagging techniques are exploited to tag the X and Higgs bosons and to reduce the dominant multijet background. Values of Y (X) mass in the range of 1 TeV to 4 TeV (50 GeV to 1000 GeV) were considered.

A search for evidence of an excess in the XH mass spectrum was made in a large number of overlapping sliding windows in the mass of the X particle. The data are found to be in agreement with the Standard Model background expectations and only small deviations are observed, with local (global) significance of no more than 2.5σ (1.2σ). Within the framework of a modified Heavy Vector Triplet model, upper limits on the resonance production cross-section $\sigma(pp \rightarrow Y \rightarrow XH \rightarrow q\bar{q}b\bar{b})$ were set at 95% CL in the two-dimensional space of the Y mass versus the X mass.

Acknowledgements

We thank CERN for the very successful operation of the LHC, as well as the support staff from our institutions without whom ATLAS could not be operated efficiently.

We acknowledge the support of ANPCyT, Argentina; YerPhI, Armenia; ARC, Australia; BMWFW and FWF, Austria; ANAS, Azerbaijan; SSTC, Belarus; CNPq and FAPESP, Brazil; NSERC, NRC and CFI, Canada; CERN; CONICYT, Chile; CAS, MOST and NSFC, China; COLCIENCIAS, Colombia; MSMT CR, MPO CR and VSC CR, Czech Republic; DNRF and DNSRC, Denmark; IN2P3-CNRS, CEA-DRF/IRFU, France; SRNSF, Georgia; BMBF, HGF, and MPG, Germany; GSRT, Greece; RGC, Hong Kong SAR, China; ISF, I-CORE and Benoziyo

Center, Israel; INFN, Italy; MEXT and JSPS, Japan; CNRST, Morocco; NWO, Netherlands; RCN, Norway; MNISW and NCN, Poland; FCT, Portugal; MNE/IFA, Romania; MES of Russia and NRC KI, Russian Federation; JINR; MESTD, Serbia; MSSR, Slovakia; ARRS and MIZŠ, Slovenia; DST/NRF, South Africa; MINECO, Spain; SRC and Wallenberg Foundation, Sweden; SERI, SNSF and Cantons of Bern and Geneva, Switzerland; MOST, Taiwan; TAEK, Turkey; STFC, United Kingdom; DOE and NSF, United States of America. In addition, individual groups and members have received support from BCKDF, the Canada Council, CANARIE, CRC, Compute Canada, FQRNT, and the Ontario Innovation Trust, Canada; EPLANET, ERC, ERDF, FP7, Horizon 2020 and Marie Skłodowska-Curie Actions, European Union; Investissements d'Avenir Labex and Idex, ANR, Région Auvergne and Fondation Partager le Savoir, France; DFG and AvH Foundation, Germany; Herakleitos, Thales and Aristeia programmes co-financed by EU-ESF and the Greek NSRF; BSF, GIF and Minerva, Israel; BRF, Norway; CERCA Programme Generalitat de Catalunya, Generalitat Valenciana, Spain; the Royal Society and Leverhulme Trust, United Kingdom.

The crucial computing support from all WLCG partners is acknowledged gratefully, in particular from CERN, the ATLAS Tier-1 facilities at TRIUMF (Canada), NDGF (Denmark, Norway, Sweden), CC-IN2P3 (France), KIT/GridKA (Germany), INFN-CNAF (Italy), NL-T1 (Netherlands), PIC (Spain), ASGC (Taiwan), RAL (UK) and BNL (USA), the Tier-2 facilities worldwide and large non-WLCG resource providers. Major contributors of computing resources are listed in Ref. [65].

References

- [1] ATLAS Collaboration, Observation of a new particle in the search for the Standard Model Higgs boson with the ATLAS detector at the LHC, *Phys. Lett. B* 716 (2012) 1, arXiv:1207.7214 [hep-ex].
- [2] CMS Collaboration, Observation of a new boson at a mass of 125 GeV with the CMS experiment at the LHC, *Phys. Lett. B* 716 (2012) 30, arXiv:1207.7235 [hep-ex].
- [3] ATLAS Collaboration, Search for new resonances decaying to a W or Z boson and a Higgs boson in the $\ell^+\ell^-b\bar{b}$, $\ell\nu b\bar{b}$, and $\nu\bar{\nu}b\bar{b}$ channels with pp collisions at $\sqrt{s} = 13$ TeV with the ATLAS detector, *Phys. Lett. B* 765 (2017) 32, arXiv:1607.05621 [hep-ex].
- [4] ATLAS Collaboration, Search for heavy resonances decaying to a W or Z boson and a Higgs boson in the $q\bar{q}(\ell\ell)b\bar{b}$ final state in pp collisions at $\sqrt{s} = 13$ TeV with the ATLAS detector, arXiv:1707.06958 [hep-ex], 2017.
- [5] CMS Collaboration, Search for heavy resonances that decay into a vector boson and a Higgs boson in hadronic final states at $\sqrt{s} = 13$ TeV, *Eur. Phys. J. C* 77 (2017) 636, arXiv:1707.01303 [hep-ex].
- [6] CMS Collaboration, Search for a massive resonance decaying into a Higgs boson and a W or Z boson in hadronic final states in proton–proton collisions at $\sqrt{s} = 8$ TeV, *J. High Energy Phys.* 02 (2016) 145, arXiv:1506.01443 [hep-ex].
- [7] CMS Collaboration, Search for massive WH resonances decaying into the $\ell\nu b\bar{b}$ final state at $\sqrt{s} = 8$ TeV, *Eur. Phys. J. C* 76 (2016) 237, arXiv:1601.06431 [hep-ex].
- [8] CMS Collaboration, Search for narrow high-mass resonances in proton–proton collisions at $\sqrt{s} = 8$ TeV decaying to a Z and a Higgs boson, *Phys. Lett. B* 748 (2015) 255, arXiv:1502.04994 [hep-ex].
- [9] ATLAS Collaboration, Search for pair production of Higgs bosons in the $b\bar{b}b\bar{b}$ final state using proton–proton collisions at $\sqrt{s} = 13$ TeV with the ATLAS detector, *Phys. Rev. D* 94 (2016) 052002, arXiv:1606.04782 [hep-ex].
- [10] CMS Collaboration, Search for heavy resonances decaying to two Higgs bosons in final states containing four b quarks, *Eur. Phys. J. C* 76 (2016) 371, arXiv:1602.08762 [hep-ex].
- [11] CMS Collaboration, Search for resonant pair production of Higgs bosons decaying to two bottom quark–antiquark pairs in proton–proton collisions at 8 TeV, *Phys. Lett. B* 749 (2015) 560, arXiv:1503.04114 [hep-ex].
- [12] ATLAS Collaboration, Search for new phenomena in dijet events using 37 fb $^{-1}$ of pp collision data collected at $\sqrt{s} = 13$ TeV with the ATLAS detector, *Phys. Rev. D* 96 (2017) 052004, arXiv:1703.09127 [hep-ex].
- [13] CMS Collaboration, Search for dijet resonances in proton–proton collisions at $\sqrt{s} = 13$ TeV and constraints on dark matter and other models, *Phys. Lett. B* 769 (2017) 520, arXiv:1611.03568 [hep-ex].
- [14] CMS Collaboration, Search for low mass vector resonances decaying into quark–antiquark pairs in proton–proton collisions at $\sqrt{s} = 13$ TeV, arXiv:1710.00159 [hep-ex], 2017.
- [15] J. Galloway, A.L. Kagan, A. Martin, A UV complete partially composite-pNGB Higgs, *Phys. Rev. D* 95 (2017) 035038, arXiv:1609.05883 [hep-ph].
- [16] U. Ellwanger, M. Rodriguez-Vazquez, Simultaneous search for extra light and heavy Higgs bosons via cascade decays, arXiv:1707.08522 [hep-ph], 2017.
- [17] K.S. Agashe, et al., LHC signals from cascade decays of warped vector resonances, *J. High Energy Phys.* 05 (2017) 078, arXiv:1612.00047 [hep-ph].
- [18] D. Pappadopulo, A. Thamm, R. Torre, A. Wulzer, Heavy vector triplets: bridging theory and data, *J. High Energy Phys.* 09 (2014) 060, arXiv:1402.4431 [hep-ph].
- [19] J. de Blas, J.M. Lizana, M. Perez-Victoria, Combining searches of Z' and W' bosons, *J. High Energy Phys.* 01 (2013) 166, arXiv:1211.2229 [hep-ph].
- [20] ATLAS Collaboration, The ATLAS experiment at the CERN Large Hadron Collider, *J. Instrum.* 3 (2008) S08003.
- [21] ATLAS Collaboration, ATLAS insertable B-layer technical design report, ATLAS-TDR-19, URL: <https://cds.cern.ch/record/1291633>; ATLAS insertable B-layer technical design report addendum, ATLAS-TDR-19-ADD-1, URL: <https://cds.cern.ch/record/1451888>.
- [22] ATLAS Collaboration, Performance of the ATLAS trigger system in 2015, *Eur. Phys. J. C* 77 (2017) 317, arXiv:1611.09661 [hep-ex].
- [23] J. Alwall, et al., The automated computation of tree-level and next-to-leading order differential cross sections, and their matching to parton shower simulations, *J. High Energy Phys.* 07 (2014) 079, arXiv:1405.0301 [hep-ph].
- [24] T. Sjöstrand, S. Mrenna, P.Z. Skands, A brief introduction to PYTHIA 8.1, *Comput. Phys. Commun.* 178 (2008) 852, arXiv:0710.3820 [hep-ph].
- [25] R.D. Ball, et al., Parton distributions with LHC data, *Nucl. Phys. B* 867 (2013) 244, arXiv:1207.1303 [hep-ph].
- [26] ATLAS Collaboration, ATLAS Pythia 8 tunes to 7 TeV data, ATL-PHYS-PUB-2014-021, URL: <https://cds.cern.ch/record/1966419>, 2014.
- [27] S. Frixione, B.R. Webber, Matching NLO QCD computations and parton shower simulations, *J. High Energy Phys.* 06 (2002) 029, arXiv:hep-ph/0204244.
- [28] H.-L. Lai, et al., New parton distributions for collider physics, *Phys. Rev. D* 82 (2010) 074024, arXiv:1007.2241 [hep-ph].
- [29] T. Sjöstrand, S. Mrenna, P.Z. Skands, PYTHIA 6.4 Physics and Manual, *J. High Energy Phys.* 05 (2006) 026, arXiv:hep-ph/0603175.
- [30] P.Z. Skands, Tuning Monte Carlo generators: the Perugia tunes, *Phys. Rev. D* 82 (2010) 074018, arXiv:1005.3457 [hep-ph].
- [31] J. Pumplin, et al., New generation of parton distributions with uncertainties from global QCD analysis, *J. High Energy Phys.* 07 (2002) 012, arXiv:hep-ph/0201195.
- [32] M. Czakon, A. Mitov, Top++: a program for the calculation of the top-pair cross-section at hadron colliders, *Comput. Phys. Commun.* 185 (2014) 2930, arXiv:1112.5675 [hep-ph].
- [33] T. Gleisberg, et al., Event generation with SHERPA 1.1, *J. High Energy Phys.* 02 (2009) 007, arXiv:0811.4622 [hep-ph].
- [34] C. Anastasiou, L.J. Dixon, K. Melnikov, F. Petriello, High precision QCD at hadron colliders: electroweak gauge boson rapidity distributions at NNLO, *Phys. Rev. D* 69 (2004) 094008, arXiv:hep-ph/0312266.
- [35] D.J. Lange, The EvtGen particle decay simulation package, *Nucl. Instrum. Methods A* 462 (2001) 152.
- [36] ATLAS Collaboration, Detector level leading track underlying event distributions at 13 TeV measured in ATLAS, ATL-PHYS-PUB-2015-019, URL: <https://cds.cern.ch/record/2037684>, 2015.
- [37] S. Agostinelli, et al., GEANT4: a simulation toolkit, *Nucl. Instrum. Methods A* 506 (2003) 250.
- [38] ATLAS Collaboration, The ATLAS simulation infrastructure, *Eur. Phys. J. C* 70 (2010) 823, arXiv:1005.4568 [hep-ex].
- [39] M. Cacciari, G.P. Salam, G. Soyez, The anti- k_t jet clustering algorithm, *J. High Energy Phys.* 04 (2008) 063, arXiv:0802.1189 [hep-ph].
- [40] M. Cacciari, G.P. Salam, G. Soyez, FastJet user manual, *Eur. Phys. J. C* 72 (2012) 1896, arXiv:1111.6097 [hep-ph].
- [41] ATLAS Collaboration, Topological cell clustering in the ATLAS calorimeters and its performance in LHC Run 1, arXiv:1603.02934 [hep-ex], 2016.
- [42] ATLAS Collaboration, Expected performance of boosted Higgs ($\rightarrow b\bar{b}$) boson identification with the ATLAS detector at $\sqrt{s} = 13$ TeV, ATL-PHYS-PUB-2015-035, URL: <https://cds.cern.ch/record/2042155>, 2015.
- [43] D. Krohn, J. Thaler, L.-T. Wang, Jet trimming, *J. High Energy Phys.* 02 (2010) 084, arXiv:0912.1342 [hep-ph].
- [44] S. Catani, Y.L. Dokshitzer, M.H. Seymour, B.R. Webber, Longitudinally invariant K_t clustering algorithms for hadron hadron collisions, *Nucl. Phys. B* 406 (1993) 187.
- [45] ATLAS Collaboration, Jet mass reconstruction with the ATLAS detector in early Run 2 data, ATLAS-CONF-2016-035, URL: <https://cds.cern.ch/record/2200211>, 2016.
- [46] ATLAS Collaboration, Muon reconstruction performance of the ATLAS detector in proton–proton collision data at $\sqrt{s} = 13$ TeV, *Eur. Phys. J. C* 76 (2016) 292, arXiv:1603.05598 [hep-ex].
- [47] ATLAS Collaboration, Boosted Higgs ($\rightarrow b\bar{b}$) boson identification with the ATLAS detector at $\sqrt{s} = 13$ TeV, ATLAS-CONF-2016-039, URL: <https://cds.cern.ch/record/2206038>, 2016.

- [48] ATLAS Collaboration, Flavor tagging with track-jets in boosted topologies with the ATLAS detector, ATL-PHYS-PUB-2014-013, URL: <https://atlas.web.cern.ch/Atlas/GROUPS/PHYSICS/PUBNOTES/ATL-PHYS-PUB-2014-013>, 2014.
- [49] ATLAS Collaboration, Optimisation of the ATLAS b -tagging performance for the 2016 LHC run, ATL-PHYS-PUB-2016-012, URL: <https://cds.cern.ch/record/2160731>, 2016.
- [50] ATLAS Collaboration, Performance of b -jet identification in the ATLAS experiment, J. Instrum. 11 (2016) P04008, arXiv:1512.01094 [hep-ex].
- [51] A.J. Larkoski, I. Moulton, D. Neill, Power counting to better jet observables, J. High Energy Phys. 12 (2014) 009, arXiv:1409.6298 [hep-ph].
- [52] A.J. Larkoski, I. Moulton, D. Neill, Analytic boosted boson discrimination, J. High Energy Phys. 05 (2016) 117, arXiv:1507.03018 [hep-ph].
- [53] ATLAS Collaboration, Performance of top quark and W boson tagging in Run 2 with ATLAS, ATLAS-CONF-2017-064, URL: <https://cds.cern.ch/record/2281054>, 2017.
- [54] ATLAS Collaboration, Identification of boosted, hadronically decaying W bosons and comparisons with ATLAS data taken at $\sqrt{s} = 8$ TeV, Eur. Phys. J. C 76 (2016) 154, arXiv:1510.05821 [hep-ex].
- [55] ATLAS Collaboration, Identification of boosted, hadronically-decaying W and Z bosons in $\sqrt{s} = 13$ TeV Monte Carlo simulations for ATLAS, ATL-PHYS-PUB-2015-033, URL: <https://cds.cern.ch/record/2041461>, 2015.
- [56] ATLAS Collaboration, Electron efficiency measurements with the ATLAS detector using the 2015 LHC proton–proton collision data, ATLAS-CONF-2016-024, URL: <https://cds.cern.ch/record/2157687>, 2016.
- [57] W. Verkerke, D. Kirkby, The RooFit toolkit for data modeling, arXiv:physics/0306116 [physics.data-an], 2003.
- [58] M. Baak, S. Gadatsch, R. Harrington, W. Verkerke, Interpolation between multi-dimensional histograms using a new non-linear moment morphing method, Nucl. Instrum. Methods A 771 (2015) 39, arXiv:1410.7388 [physics.data-an].
- [59] ATLAS Collaboration, Jet energy measurement and its systematic uncertainty in proton–proton collisions at $\sqrt{s} = 7$ TeV with the ATLAS detector, Eur. Phys. J. C 75 (2015) 17, arXiv:1406.0076 [hep-ex].
- [60] ATLAS Collaboration, Measurement of the differential cross-section of highly boosted top quarks as a function of their transverse momentum in $\sqrt{s} = 8$ TeV proton–proton collisions using the ATLAS detector, Phys. Rev. D 93 (2016) 032009, arXiv:1510.03818 [hep-ex].
- [61] ATLAS Collaboration, Luminosity determination in pp collisions at $\sqrt{s} = 8$ TeV using the ATLAS detector at the LHC, Eur. Phys. J. C 76 (2016) 653, arXiv:1608.03953 [hep-ex].
- [62] ATLAS Collaboration, Performance of jet substructure techniques for large- R jets in proton–proton collisions at $\sqrt{s} = 7$ TeV using the ATLAS detector, J. High Energy Phys. 09 (2013) 076, arXiv:1306.4945 [hep-ex].
- [63] Glen Cowan, Kyle Cranmer, Eilam Gross, Ofer Vitells, Asymptotic formulae for likelihood-based tests of new physics, Eur. Phys. J. C 71 (2011) 1554, arXiv:1007.1727 [physics.data-an], Erratum: Eur. Phys. J. C 73 (2013) 2501.
- [64] A.L. Read, Presentation of search results: the CL(s) technique, J. Phys. G 28 (2002) 2693.
- [65] ATLAS Collaboration, ATLAS computing acknowledgements 2016–2017, ATLAS-CONF-2016-002, URL: <https://cds.cern.ch/record/2202407>.

The ATLAS Collaboration

M. Aaboud^{137d}, G. Aad⁸⁸, B. Abbott¹¹⁵, O. Abdinov^{12,*}, B. Abeloos¹¹⁹, S.H. Abidi¹⁶¹, O.S. AbouZeid¹³⁹, N.L. Abraham¹⁵¹, H. Abramowicz¹⁵⁵, H. Abreu¹⁵⁴, R. Abreu¹¹⁸, Y. Abulaiti^{148a,148b}, B.S. Acharya^{167a,167b,a}, S. Adachi¹⁵⁷, L. Adamczyk^{41a}, J. Adelman¹¹⁰, M. Adersberger¹⁰², T. Adye¹³³, A.A. Affolder¹³⁹, Y. Afik¹⁵⁴, C. Agheorghiesei^{28c}, J.A. Aguilar-Saavedra^{128a,128f}, S.P. Ahlen²⁴, F. Ahmadov^{68,b}, G. Aielli^{135a,135b}, S. Akatsuka⁷¹, H. Akerstedt^{148a,148b}, T.P.A. Åkesson⁸⁴, E. Akilli⁵², A.V. Akimov⁹⁸, G.L. Alberghi^{22a,22b}, J. Albert¹⁷², P. Albicocco⁵⁰, M.J. Alconada Verzini⁷⁴, S.C. Alderweireldt¹⁰⁸, M. Aleksa³², I.N. Aleksandrov⁶⁸, C. Alexa^{28b}, G. Alexander¹⁵⁵, T. Alexopoulos¹⁰, M. Alhroob¹¹⁵, B. Ali¹³⁰, M. Aliev^{76a,76b}, G. Alimonti^{94a}, J. Alison³³, S.P. Alkire³⁸, B.M.M. Allbrooke¹⁵¹, B.W. Allen¹¹⁸, P.P. Allport¹⁹, A. Aloisio^{106a,106b}, A. Alonso³⁹, F. Alonso⁷⁴, C. Alpigiani¹⁴⁰, A.A. Alshehri⁵⁶, M.I. Alstamy⁸⁸, B. Alvarez Gonzalez³², D. Álvarez Piqueras¹⁷⁰, M.G. Alviggi^{106a,106b}, B.T. Amadio¹⁶, Y. Amaral Coutinho^{26a}, C. Amelung²⁵, D. Amidei⁹², S.P. Amor Dos Santos^{128a,128c}, S. Amoroso³², C. Anastopoulos¹⁴¹, L.S. Ancu⁵², N. Andari¹⁹, T. Andeen¹¹, C.F. Anders^{60b}, J.K. Anders⁷⁷, K.J. Anderson³³, A. Andreazza^{94a,94b}, V. Andrei^{60a}, S. Angelidakis³⁷, I. Angelozzi¹⁰⁹, A. Angerami³⁸, A.V. Anisenkov^{111,c}, N. Anjos¹³, A. Annovi^{126a,126b}, C. Antel^{60a}, M. Antonelli⁵⁰, A. Antonov^{100,*}, D.J. Antrim¹⁶⁶, F. Anulli^{134a}, M. Aoki⁶⁹, L. Aperio Bella³², G. Arabidze⁹³, Y. Arai⁶⁹, J.P. Araque^{128a}, V. Araujo Ferraz^{26a}, A.T.H. Arce⁴⁸, R.E. Ardell⁸⁰, F.A. Arduh⁷⁴, J-F. Arguin⁹⁷, S. Argyropoulos⁶⁶, M. Arik^{20a}, A.J. Armbruster³², L.J. Armitage⁷⁹, O. Arnaez¹⁶¹, H. Arnold⁵¹, M. Arratia³⁰, O. Arslan²³, A. Artamonov^{99,*}, G. Artoni¹²², S. Artz⁸⁶, S. Asai¹⁵⁷, N. Asbah⁴⁵, A. Ashkenazi¹⁵⁵, L. Asquith¹⁵¹, K. Assamagan²⁷, R. Astalos^{146a}, M. Atkinson¹⁶⁹, N.B. Atlay¹⁴³, K. Augsten¹³⁰, G. Avolio³², B. Axen¹⁶, M.K. Ayoub^{35a}, G. Azuelos^{97,d}, A.E. Baas^{60a}, M.J. Baca¹⁹, H. Bachacou¹³⁸, K. Bachas^{76a,76b}, M. Backes¹²², P. Bagnaia^{134a,134b}, M. Bahmani⁴², H. Bahrasemani¹⁴⁴, J.T. Baines¹³³, M. Bajic³⁹, O.K. Baker¹⁷⁹, P.J. Bakker¹⁰⁹, E.M. Baldin^{111,c}, P. Balek¹⁷⁵, F. Balli¹³⁸, W.K. Balunas¹²⁴, E. Banas⁴², A. Bandyopadhyay²³, Sw. Banerjee^{176,e}, A.A.E. Bannoura¹⁷⁸, L. Barak¹⁵⁵, E.L. Barberio⁹¹, D. Barberis^{53a,53b}, M. Barbero⁸⁸, T. Barillari¹⁰³, M-S Barisits⁶⁵, J.T. Barkeloo¹¹⁸, T. Barklow¹⁴⁵, N. Barlow³⁰, S.L. Barnes^{36c}, B.M. Barnett¹³³, R.M. Barnett¹⁶, Z. Barnovska-Blenessy^{36a}, A. Baroncelli^{136a}, G. Barone²⁵, A.J. Barr¹²², L. Barranco Navarro¹⁷⁰, F. Barreiro⁸⁵, J. Barreiro Guimarães da Costa^{35a}, R. Bartoldus¹⁴⁵, A.E. Barton⁷⁵, P. Bartos^{146a}, A. Basalaev¹²⁵, A. Bassalat^{119,f}, R.L. Bates⁵⁶, S.J. Batista¹⁶¹, J.R. Batley³⁰, M. Battaglia¹³⁹, M. Bause^{134a,134b}, F. Bauer¹³⁸, K.T. Bauer¹⁶⁶, H.S. Bawa^{145,g}, J.B. Beacham¹¹³, M.D. Beattie⁷⁵, T. Beau⁸³, P.H. Beauchemin¹⁶⁵, P. Bechtel²³, H.P. Beck^{18,h}, H.C. Beck⁵⁷, K. Becker¹²², M. Becker⁸⁶, C. Becot¹¹², A.J. Beddall^{20e}, A. Beddall^{20b}, V.A. Bednyakov⁶⁸, M. Bedognetti¹⁰⁹, C.P. Bee¹⁵⁰, T.A. Beermann³², M. Begalli^{26a}, M. Begel²⁷, J.K. Behr⁴⁵, A.S. Bell⁸¹, G. Bella¹⁵⁵, L. Bellagamba^{22a}, A. Bellerive³¹, M. Bellomo¹⁵⁴, K. Belotskiy¹⁰⁰, O. Beltramello³², N.L. Belyaev¹⁰⁰, O. Benary^{155,*}, D. Bencheikroun^{137a}, M. Bender¹⁰², N. Benekos¹⁰, Y. Benhammou¹⁵⁵,

E. Benhar Noccioli ¹⁷⁹, J. Benitez ⁶⁶, D.P. Benjamin ⁴⁸, M. Benoit ⁵², J.R. Bensinger ²⁵, S. Bentvelsen ¹⁰⁹, L. Beresford ¹²², M. Beretta ⁵⁰, D. Berge ¹⁰⁹, E. Bergeaas Kuutmann ¹⁶⁸, N. Berger ⁵, L.J. Bergsten ²⁵, J. Beringer ¹⁶, S. Berlendis ⁵⁸, N.R. Bernard ⁸⁹, G. Bernardi ⁸³, C. Bernius ¹⁴⁵, F.U. Bernlochner ²³, T. Berry ⁸⁰, P. Berta ⁸⁶, C. Bertella ^{35a}, G. Bertoli ^{148a,148b}, I.A. Bertram ⁷⁵, C. Bertsche ⁴⁵, G.J. Besjes ³⁹, O. Bessidskaia Bylund ^{148a,148b}, M. Bessner ⁴⁵, N. Besson ¹³⁸, A. Bethani ⁸⁷, S. Bethke ¹⁰³, A. Betti ²³, A.J. Bevan ⁷⁹, J. Beyer ¹⁰³, R.M. Bianchi ¹²⁷, O. Biebel ¹⁰², D. Biedermann ¹⁷, R. Bielski ⁸⁷, K. Bierwagen ⁸⁶, N.V. Biesuz ^{126a,126b}, M. Biglietti ^{136a}, T.R.V. Billoud ⁹⁷, H. Bilokon ⁵⁰, M. Bindi ⁵⁷, A. Bingul ^{20b}, C. Bini ^{134a,134b}, S. Biondi ^{22a,22b}, T. Bisanz ⁵⁷, C. Bittrich ⁴⁷, D.M. Bjergaard ⁴⁸, J.E. Black ¹⁴⁵, K.M. Black ²⁴, R.E. Blair ⁶, T. Blazek ^{146a}, I. Bloch ⁴⁵, C. Blocker ²⁵, A. Blue ⁵⁶, U. Blumenschein ⁷⁹, S. Blunier ^{34a}, G.J. Bobbink ¹⁰⁹, V.S. Bobrovnikov ^{111,c}, S.S. Bocchetta ⁸⁴, A. Bocci ⁴⁸, C. Bock ¹⁰², M. Boehler ⁵¹, D. Boerner ¹⁷⁸, D. Bogavac ¹⁰², A.G. Bogdanchikov ¹¹¹, C. Bohm ^{148a}, V. Boisvert ⁸⁰, P. Bokan ^{168,i}, T. Bold ^{41a}, A.S. Boldyrev ¹⁰¹, A.E. Bolz ^{60b}, M. Bomben ⁸³, M. Bona ⁷⁹, M. Boonekamp ¹³⁸, A. Borisov ¹³², G. Borissov ⁷⁵, J. Bortfeldt ³², D. Bortoletto ¹²², V. Bortolotto ^{62a}, D. Boscherini ^{22a}, M. Bosman ¹³, J.D. Bossio Sola ²⁹, J. Boudreau ¹²⁷, E.V. Bouhova-Thacker ⁷⁵, D. Boumediene ³⁷, C. Bourdarios ¹¹⁹, S.K. Boutle ⁵⁶, A. Boveia ¹¹³, J. Boyd ³², I.R. Boyko ⁶⁸, A.J. Bozson ⁸⁰, J. Bracinik ¹⁹, A. Brandt ⁸, G. Brandt ⁵⁷, O. Brandt ^{60a}, F. Braren ⁴⁵, U. Bratzler ¹⁵⁸, B. Brau ⁸⁹, J.E. Brau ¹¹⁸, W.D. Breaden Madden ⁵⁶, K. Brendlinger ⁴⁵, A.J. Brennan ⁹¹, L. Brenner ¹⁰⁹, R. Brenner ¹⁶⁸, S. Bressler ¹⁷⁵, D.L. Briglin ¹⁹, T.M. Bristow ⁴⁹, D. Britton ⁵⁶, D. Britzger ⁴⁵, F.M. Brochu ³⁰, I. Brock ²³, R. Brock ⁹³, G. Brooijmans ³⁸, T. Brooks ⁸⁰, W.K. Brooks ^{34b}, E. Brost ¹¹⁰, J.H. Broughton ¹⁹, P.A. Bruckman de Renstrom ⁴², D. Bruncko ^{146b}, A. Bruni ^{22a}, G. Bruni ^{22a}, L.S. Bruni ¹⁰⁹, S. Bruno ^{135a,135b}, B.H. Brunt ³⁰, M. Bruschi ^{22a}, N. Bruscino ¹²⁷, P. Bryant ³³, L. Bryngemark ⁴⁵, T. Buanes ¹⁵, Q. Buat ¹⁴⁴, P. Buchholz ¹⁴³, A.G. Buckley ⁵⁶, I.A. Budagov ⁶⁸, F. Buehrer ⁵¹, M.K. Bugge ¹²¹, O. Bulekov ¹⁰⁰, D. Bullock ⁸, T.J. Burch ¹¹⁰, S. Burdin ⁷⁷, C.D. Burgard ¹⁰⁹, A.M. Burger ⁵, B. Burghgrave ¹¹⁰, K. Burka ⁴², S. Burke ¹³³, I. Burmeister ⁴⁶, J.T.P. Burr ¹²², D. Büscher ⁵¹, V. Büscher ⁸⁶, P. Bussey ⁵⁶, J.M. Butler ²⁴, C.M. Buttar ⁵⁶, J.M. Butterworth ⁸¹, P. Butti ³², W. Buttinger ²⁷, A. Buzatu ¹⁵³, A.R. Buzykaev ^{111,c}, C.-Q. Changqiao ^{36a}, S. Cabrera Urbán ¹⁷⁰, D. Caforio ¹³⁰, H. Cai ¹⁶⁹, V.M. Cairo ^{40a,40b}, O. Cakir ^{4a}, N. Calace ⁵², P. Calafiura ¹⁶, A. Calandri ⁸⁸, G. Calderini ⁸³, P. Calfayan ⁶⁴, G. Callea ^{40a,40b}, L.P. Caloba ^{26a}, S. Calvente Lopez ⁸⁵, D. Calvet ³⁷, S. Calvet ³⁷, T.P. Calvet ⁸⁸, R. Camacho Toro ³³, S. Camarda ³², P. Camarri ^{135a,135b}, D. Cameron ¹²¹, R. Caminal Armadans ¹⁶⁹, C. Camincher ⁵⁸, S. Campana ³², M. Campanelli ⁸¹, A. Camplani ^{94a,94b}, A. Campoverde ¹⁴³, V. Canale ^{106a,106b}, M. Cano Bret ^{36c}, J. Cantero ¹¹⁶, T. Cao ¹⁵⁵, M.D.M. Capeans Garrido ³², I. Caprini ^{28b}, M. Caprini ^{28b}, M. Capua ^{40a,40b}, R.M. Carbone ³⁸, R. Cardarelli ^{135a}, F. Cardillo ⁵¹, I. Carli ¹³¹, T. Carli ³², G. Carlino ^{106a}, B.T. Carlson ¹²⁷, L. Carminati ^{94a,94b}, R.M.D. Carney ^{148a,148b}, S. Caron ¹⁰⁸, E. Carquin ^{34b}, S. Carrá ^{94a,94b}, G.D. Carrillo-Montoya ³², D. Casadei ¹⁹, M.P. Casado ^{13,j}, A.F. Casha ¹⁶¹, M. Casolino ¹³, D.W. Casper ¹⁶⁶, R. Castelijns ¹⁰⁹, V. Castillo Gimenez ¹⁷⁰, N.F. Castro ^{128a,k}, A. Catinaccio ³², J.R. Catmore ¹²¹, A. Cattai ³², J. Caudron ²³, V. Cavaliere ¹⁶⁹, E. Cavallaro ¹³, D. Cavalli ^{94a}, M. Cavalli-Sforza ¹³, V. Cavasinni ^{126a,126b}, E. Celebi ^{20d}, F. Ceradini ^{136a,136b}, L. Cerda Alberich ¹⁷⁰, A.S. Cerqueira ^{26b}, A. Cerri ¹⁵¹, L. Cerrito ^{135a,135b}, F. Cerutti ¹⁶, A. Cervelli ^{22a,22b}, S.A. Cetin ^{20d}, A. Chafaq ^{137a}, D. Chakraborty ¹¹⁰, S.K. Chan ⁵⁹, W.S. Chan ¹⁰⁹, Y.L. Chan ^{62a}, P. Chang ¹⁶⁹, J.D. Chapman ³⁰, D.G. Charlton ¹⁹, C.C. Chau ³¹, C.A. Chavez Barajas ¹⁵¹, S. Che ¹¹³, S. Cheatham ^{167a,167c}, A. Chegwidden ⁹³, S. Chekanov ⁶, S.V. Chekulaev ^{163a}, G.A. Chelkov ^{68,l}, M.A. Chelstowska ³², C. Chen ^{36a}, C. Chen ⁶⁷, H. Chen ²⁷, J. Chen ^{36a}, S. Chen ^{35b}, S. Chen ¹⁵⁷, X. Chen ^{35c,m}, Y. Chen ⁷⁰, H.C. Cheng ⁹², H.J. Cheng ^{35a,35d}, A. Cheplakov ⁶⁸, E. Cheremushkina ¹³², R. Cherkaoui El Moursli ^{137e}, E. Cheu ⁷, K. Cheung ⁶³, L. Chevalier ¹³⁸, V. Chiarella ⁵⁰, G. Chiarelli ^{126a,126b}, G. Chiodini ^{76a}, A.S. Chisholm ³², A. Chitan ^{28b}, Y.H. Chiu ¹⁷², M.V. Chizhov ⁶⁸, K. Choi ⁶⁴, A.R. Chomont ³⁷, S. Chouridou ¹⁵⁶, Y.S. Chow ^{62a}, V. Christodoulou ⁸¹, M.C. Chu ^{62a}, J. Chudoba ¹²⁹, A.J. Chuinard ⁹⁰, J.J. Chwastowski ⁴², L. Chytka ¹¹⁷, A.K. Ciftci ^{4a}, D. Cinca ⁴⁶, V. Cindro ⁷⁸, I.A. Cioara ²³, A. Ciocio ¹⁶, F. Ciotto ^{106a,106b}, Z.H. Citron ¹⁷⁵, M. Citterio ^{94a}, M. Ciubancan ^{28b}, A. Clark ⁵², M.R. Clark ³⁸, P.J. Clark ⁴⁹, R.N. Clarke ¹⁶, C. Clement ^{148a,148b}, Y. Coadou ⁸⁸, M. Cobl ^{167a,167c}, A. Coccaro ⁵², J. Cochran ⁶⁷, L. Colasurdo ¹⁰⁸, B. Cole ³⁸, A.P. Colijn ¹⁰⁹, J. Collot ⁵⁸, T. Colombo ¹⁶⁶, P. Conde Muiño ^{128a,128b}, E. Coniavitis ⁵¹, S.H. Connell ^{147b}, I.A. Connelly ⁸⁷, S. Constantinescu ^{28b}, G. Conti ³², F. Conventi ^{106a,n}, M. Cooke ¹⁶, A.M. Cooper-Sarkar ¹²², F. Cormier ¹⁷¹, K.J.R. Cormier ¹⁶¹, M. Corradi ^{134a,134b}, E.E. Corrigan ⁸⁴, F. Corriveau ^{90,o}, A. Cortes-Gonzalez ³², G. Costa ^{94a}, M.J. Costa ¹⁷⁰, D. Costanzo ¹⁴¹, G. Cottin ³⁰, G. Cowan ⁸⁰, B.E. Cox ⁸⁷, K. Cranmer ¹¹²,

S.J. Crawley⁵⁶, R.A. Creager¹²⁴, G. Cree³¹, S. Crépé-Renaudin⁵⁸, F. Crescioli⁸³, W.A. Cribbs^{148a,148b}, M. Cristinziani²³, V. Croft¹¹², G. Crosetti^{40a,40b}, A. Cueto⁸⁵, T. Cuhadar Donszelmann¹⁴¹, A.R. Cukierman¹⁴⁵, J. Cummings¹⁷⁹, M. Curatolo⁵⁰, J. Cúth⁸⁶, S. Czekerda⁴², P. Czodrowski³², G. D'amen^{22a,22b}, S. D'Auria⁵⁶, L. D'eraimo⁸³, M. D'Onofrio⁷⁷, M.J. Da Cunha Sargedas De Sousa^{128a,128b}, C. Da Via⁸⁷, W. Dabrowski^{41a}, T. Dado^{146a}, T. Dai⁹², O. Dale¹⁵, F. Dallaire⁹⁷, C. Dallapiccola⁸⁹, M. Dam³⁹, J.R. Dandoy¹²⁴, M.F. Daneri²⁹, N.P. Dang¹⁷⁶, A.C. Daniells¹⁹, N.S. Dann⁸⁷, M. Danninger¹⁷¹, M. Dano Hoffmann¹³⁸, V. Dao¹⁵⁰, G. Darbo^{53a}, S. Darmora⁸, J. Dassoulas³, A. Dattagupta¹¹⁸, T. Daubney⁴⁵, W. Davey²³, C. David⁴⁵, T. Davidek¹³¹, D.R. Davis⁴⁸, P. Davison⁸¹, E. Dawe⁹¹, I. Dawson¹⁴¹, K. De⁸, R. de Asmundis^{106a}, A. De Benedetti¹¹⁵, S. De Castro^{22a,22b}, S. De Cecco⁸³, N. De Groot¹⁰⁸, P. de Jong¹⁰⁹, H. De la Torre⁹³, F. De Lorenzi⁶⁷, A. De Maria⁵⁷, D. De Pedis^{134a}, A. De Salvo^{134a}, U. De Sanctis^{135a,135b}, A. De Santo¹⁵¹, K. De Vasconcelos Corga⁸⁸, J.B. De Vivie De Regie¹¹⁹, R. Debbe²⁷, C. Debenedetti¹³⁹, D.V. Dedovich⁶⁸, N. Dehghanian³, I. Deigaard¹⁰⁹, M. Del Gaudio^{40a,40b}, J. Del Peso⁸⁵, D. Delgove¹¹⁹, F. Deliot¹³⁸, C.M. Delitzsch⁷, A. Dell'Acqua³², L. Dell'Asta²⁴, M. Dell'Orso^{126a,126b}, M. Della Pietra^{106a,106b}, D. della Volpe⁵², M. Delmastro⁵, C. Delporte¹¹⁹, P.A. Delsart⁵⁸, D.A. DeMarco¹⁶¹, S. Demers¹⁷⁹, M. Demichev⁶⁸, A. Demilly⁸³, S.P. Denisov¹³², D. Denysiuk¹³⁸, D. Derendarz⁴², J.E. Derkaoui^{137d}, F. Derue⁸³, P. Dervan⁷⁷, K. Desch²³, C. Deterre⁴⁵, K. Dette¹⁶¹, M.R. Devesa²⁹, P.O. Deviveiros³², A. Dewhurst¹³³, S. Dhaliwal²⁵, F.A. Di Bello⁵², A. Di Ciaccio^{135a,135b}, L. Di Ciaccio⁵, W.K. Di Clemente¹²⁴, C. Di Donato^{106a,106b}, A. Di Girolamo³², B. Di Girolamo³², B. Di Micco^{136a,136b}, R. Di Nardo³², K.F. Di Petrillo⁵⁹, A. Di Simone⁵¹, R. Di Sipio¹⁶¹, D. Di Valentino³¹, C. Diaconu⁸⁸, M. Diamond¹⁶¹, F.A. Dias³⁹, M.A. Diaz^{34a}, E.B. Diehl⁹², J. Dietrich¹⁷, S. Díez Cornell⁴⁵, A. Dimitrievska¹⁴, J. Dingfelder²³, P. Dita^{28b}, S. Dita^{28b}, F. Dittus³², F. Djama⁸⁸, T. Djobava^{54b}, J.I. Djuvsland^{60a}, M.A.B. do Vale^{26c}, M. Dobre^{28b}, D. Dodsworth²⁵, C. Doglioni⁸⁴, J. Dolejsi¹³¹, Z. Dolezal¹³¹, M. Donadelli^{26d}, S. Donati^{126a,126b}, J. Donini³⁷, J. Dopke¹³³, A. Doria^{106a}, M.T. Dova⁷⁴, A.T. Doyle⁵⁶, E. Drechsler⁵⁷, M. Dris¹⁰, Y. Du^{36b}, J. Duarte-Campderros¹⁵⁵, F. Dubinin⁹⁸, A. Dubreuil⁵², E. Duchovni¹⁷⁵, G. Duckeck¹⁰², A. Ducourthial⁸³, O.A. Ducu^{97,p}, D. Duda¹⁰⁹, A. Dudarev³², A. Chr. Dudder⁸⁶, E.M. Duffield¹⁶, L. Duflot¹¹⁹, M. Dührssen³², C. Dulsen¹⁷⁸, M. Dumancic¹⁷⁵, A.E. Dumitriu^{28b}, A.K. Duncan⁵⁶, M. Dunford^{60a}, A. Duperrin⁸⁸, H. Duran Yildiz^{4a}, M. Düren⁵⁵, A. Durglishvili^{54b}, D. Duschinger⁴⁷, B. Dutta⁴⁵, D. Duvnjak¹, M. Dyndal⁴⁵, B.S. Dziedzic⁴², C. Eckardt⁴⁵, K.M. Ecker¹⁰³, R.C. Edgar⁹², T. Eifert³², G. Eigen¹⁵, K. Einsweiler¹⁶, T. Ekelof¹⁶⁸, M. El Kacimi^{137c}, R. El Kosseifi⁸⁸, V. Ellajosyula⁸⁸, M. Ellert¹⁶⁸, S. Elles⁵, F. Ellinghaus¹⁷⁸, A.A. Elliot¹⁷², N. Ellis³², J. Elmsheuser²⁷, M. Elsing³², D. Emeliyanov¹³³, A. Emerman³⁸, Y. Enari¹⁵⁷, J.S. Ennis¹⁷³, M.B. Epland⁴⁸, J. Erdmann⁴⁶, A. Ereditato¹⁸, M. Ernst²⁷, S. Errede¹⁶⁹, M. Escalier¹¹⁹, C. Escobar¹⁷⁰, B. Esposito⁵⁰, O. Estrada Pastor¹⁷⁰, A.I. Etienvre¹³⁸, E. Etzion¹⁵⁵, H. Evans⁶⁴, A. Ezhilov¹²⁵, M. Ezzi^{137e}, F. Fabbri^{22a,22b}, L. Fabbri^{22a,22b}, V. Fabiani¹⁰⁸, G. Facini⁸¹, R.M. Fakhruddinov¹³², S. Falciano^{134a}, R.J. Falla⁸¹, J. Faltova³², Y. Fang^{35a}, M. Fanti^{94a,94b}, A. Farbin⁸, A. Farilla^{136a}, E.M. Farina^{123a,123b}, T. Farooque⁹³, S. Farrell¹⁶, S.M. Farrington¹⁷³, P. Farthouat³², F. Fassi^{137e}, P. Fassnacht³², D. Fassouliotis⁹, M. Faucci Giannelli⁴⁹, A. Favareto^{53a,53b}, W.J. Fawcett¹²², L. Fayard¹¹⁹, O.L. Fedin^{125,q}, W. Fedorko¹⁷¹, S. Feigl¹²¹, L. Feligioni⁸⁸, C. Feng^{36b}, E.J. Feng³², M. Feng⁴⁸, M.J. Fenton⁵⁶, A.B. Fenyuk¹³², L. Feremenga⁸, P. Fernandez Martinez¹⁷⁰, J. Ferrando⁴⁵, A. Ferrari¹⁶⁸, P. Ferrari¹⁰⁹, R. Ferrari^{123a}, D.E. Ferreira de Lima^{60b}, A. Ferrer¹⁷⁰, D. Ferrere⁵², C. Ferretti⁹², F. Fiedler⁸⁶, A. Filipčič⁷⁸, M. Filipuzzi⁴⁵, F. Filthaut¹⁰⁸, M. Fincke-Keeler¹⁷², K.D. Finelli²⁴, M.C.N. Fiolhais^{128a,128c,r}, L. Fiorini¹⁷⁰, A. Fischer², C. Fischer¹³, J. Fischer¹⁷⁸, W.C. Fisher⁹³, N. Flaschel⁴⁵, I. Fleck¹⁴³, P. Fleischmann⁹², R.R.M. Fletcher¹²⁴, T. Flick¹⁷⁸, B.M. Flierl¹⁰², L.R. Flores Castillo^{62a}, M.J. Flowerdew¹⁰³, G.T. Forcolin⁸⁷, A. Formica¹³⁸, F.A. Förster¹³, A. Forti⁸⁷, A.G. Foster¹⁹, D. Fournier¹¹⁹, H. Fox⁷⁵, S. Fracchia¹⁴¹, P. Francavilla^{126a,126b}, M. Franchini^{22a,22b}, S. Franchino^{60a}, D. Francis³², L. Franconi¹²¹, M. Franklin⁵⁹, M. Frate¹⁶⁶, M. Fraternali^{123a,123b}, D. Freeborn⁸¹, S.M. Fressard-Batraneanu³², B. Freund⁹⁷, D. Froidevaux³², J.A. Frost¹²², C. Fukunaga¹⁵⁸, T. Fusayasu¹⁰⁴, J. Fuster¹⁷⁰, O. Gabizon¹⁵⁴, A. Gabrielli^{22a,22b}, A. Gabrielli¹⁶, G.P. Gach^{41a}, S. Gadatsch³², S. Gadomski⁸⁰, G. Gagliardi^{53a,53b}, L.G. Gagnon⁹⁷, C. Galea¹⁰⁸, B. Galhardo^{128a,128c}, E.J. Gallas¹²², B.J. Gallop¹³³, P. Gallus¹³⁰, G. Galster³⁹, K.K. Gan¹¹³, S. Ganguly³⁷, Y. Gao⁷⁷, Y.S. Gao^{145,g}, F.M. Garay Walls^{34a}, C. García¹⁷⁰, J.E. García Navarro¹⁷⁰, J.A. García Pascual^{35a}, M. Garcia-Sciveres¹⁶, R.W. Gardner³³, N. Garelli¹⁴⁵,

V. Garonne¹²¹, A. Gascon Bravo⁴⁵, K. Gasnikova⁴⁵, C. Gatti⁵⁰, A. Gaudiello^{53a,53b}, G. Gaudio^{123a}, I.L. Gavrilenko⁹⁸, C. Gay¹⁷¹, G. Gaycken²³, E.N. Gazis¹⁰, C.N.P. Gee¹³³, J. Geisen⁵⁷, M. Geisen⁸⁶, M.P. Geisler^{60a}, K. Gellerstedt^{148a,148b}, C. Gemme^{53a}, M.H. Genest⁵⁸, C. Geng⁹², S. Gentile^{134a,134b}, C. Gentsos¹⁵⁶, S. George⁸⁰, D. Gerbaudo¹³, G. Geßner⁴⁶, S. Ghasemi¹⁴³, M. Ghneimat²³, B. Giacobbe^{22a}, S. Giagu^{134a,134b}, N. Giangiacomi^{22a,22b}, P. Giannetti^{126a,126b}, S.M. Gibson⁸⁰, M. Gignac¹⁷¹, M. Gilchriese¹⁶, D. Gillberg³¹, G. Gilles¹⁷⁸, D.M. Gingrich^{3,d}, M.P. Giordani^{167a,167c}, F.M. Giorgi^{22a}, P.F. Giraud¹³⁸, P. Giromini⁵⁹, G. Giugliarelli^{167a,167c}, D. Giugni^{94a}, F. Giuli¹²², C. Giuliani¹⁰³, M. Giulini^{60b}, B.K. Gjelsten¹²¹, S. Gkaitatzis¹⁵⁶, I. Gkialas^{9,s}, E.L. Gkougkousis¹³, P. Gkoutoumis¹⁰, L.K. Gladilin¹⁰¹, C. Glasman⁸⁵, J. Glatzer¹³, P.C.F. Glaysheer⁴⁵, A. Glazov⁴⁵, M. Goblirsch-Kolb²⁵, J. Godlewski⁴², S. Goldfarb⁹¹, T. Golling⁵², D. Golubkov¹³², A. Gomes^{128a,128b,128d}, R. Gonçalo^{128a}, R. Goncalves Gama^{26a}, J. Goncalves Pinto Firmino Da Costa¹³⁸, G. Gonella⁵¹, L. Gonella¹⁹, A. Gongadze⁶⁸, J.L. Gonski⁵⁹, S. González de la Hoz¹⁷⁰, S. Gonzalez-Sevilla⁵², L. Goossens³², P.A. Gorbounov⁹⁹, H.A. Gordon²⁷, B. Gorini³², E. Gorini^{76a,76b}, A. Gorišek⁷⁸, A.T. Goshaw⁴⁸, C. Gössling⁴⁶, M.I. Gostkin⁶⁸, C.A. Gottardo²³, C.R. Goudet¹¹⁹, D. Goujdami^{137c}, A.G. Goussiou¹⁴⁰, N. Govender^{147b,t}, E. Gozani¹⁵⁴, I. Grabowska-Bold^{41a}, P.O.J. Gradin¹⁶⁸, E.C. Graham⁷⁷, J. Gramling¹⁶⁶, E. Gramstad¹²¹, S. Grancagnolo¹⁷, V. Gratchev¹²⁵, P.M. Gravila^{28f}, C. Gray⁵⁶, H.M. Gray¹⁶, Z.D. Greenwood^{82,u}, C. Grefe²³, K. Gregersen⁸¹, I.M. Gregor⁴⁵, P. Grenier¹⁴⁵, K. Grevtsov⁵, J. Griffiths⁸, A.A. Grillo¹³⁹, K. Grimm⁷⁵, S. Grinstein^{13,v}, Ph. Gris³⁷, J.-F. Grivaz¹¹⁹, S. Groh⁸⁶, E. Gross¹⁷⁵, J. Grosse-Knetter⁵⁷, G.C. Grossi⁸², Z.J. Grout⁸¹, A. Grummer¹⁰⁷, L. Guan⁹², W. Guan¹⁷⁶, J. Guenther³², F. Guescini^{163a}, D. Guest¹⁶⁶, O. Gueta¹⁵⁵, B. Gui¹¹³, E. Guido^{53a,53b}, T. Guillemain⁵, S. Guindon³², U. Gul⁵⁶, C. Gumpert³², J. Guo^{36c}, W. Guo⁹², Y. Guo^{36a,w}, R. Gupta⁴³, S. Gurbuz^{20a}, G. Gustavino¹¹⁵, B.J. Gutelman¹⁵⁴, P. Gutierrez¹¹⁵, N.G. Gutierrez Ortiz⁸¹, C. Gutsche⁸¹, C. Guyot¹³⁸, M.P. Guzik^{41a}, C. Gwenlan¹²², C.B. Gwilliam⁷⁷, A. Haas¹¹², C. Haber¹⁶, H.K. Hadavand⁸, N. Haddad^{137e}, A. Hadeef⁸⁸, S. Hageböck²³, M. Hagihara¹⁶⁴, H. Hakobyan^{180,*}, M. Haleem⁴⁵, J. Haley¹¹⁶, G. Halladjian⁹³, G.D. Hallowell⁸⁸, K. Hamacher¹⁷⁸, P. Hamal¹¹⁷, K. Hamano¹⁷², A. Hamilton^{147a}, G.N. Hamity¹⁴¹, P.G. Hamnett⁴⁵, K. Han^{36a,x}, L. Han^{36a}, S. Han^{35a,35d}, K. Hanagaki^{69,y}, K. Hanawa¹⁵⁷, M. Hance¹³⁹, D.M. Handl¹⁰², B. Haney¹²⁴, P. Hanke^{60a}, J.B. Hansen³⁹, J.D. Hansen³⁹, M.C. Hansen²³, P.H. Hansen³⁹, K. Hara¹⁶⁴, A.S. Hard¹⁷⁶, T. Harenberg¹⁷⁸, F. Hariri¹¹⁹, S. Harkusha⁹⁵, P.F. Harrison¹⁷³, N.M. Hartmann¹⁰², Y. Hasegawa¹⁴², A. Hasib⁴⁹, S. Hassani¹³⁸, S. Haug¹⁸, R. Hauser⁹³, L. Hauswald⁴⁷, L.B. Havener³⁸, M. Havranek¹³⁰, C.M. Hawkes¹⁹, R.J. Hawking³², D. Hayden⁹³, C.P. Hays¹²², J.M. Hays⁷⁹, H.S. Hayward⁷⁷, S.J. Haywood¹³³, T. Heck⁸⁶, V. Hedberg⁸⁴, L. Heelan⁸, S. Heer²³, K.K. Heidegger⁵¹, S. Heim⁴⁵, T. Heim¹⁶, B. Heinemann^{45,z}, J.J. Heinrich¹⁰², L. Heinrich¹¹², C. Heinz⁵⁵, J. Hejbal¹²⁹, L. Helary³², A. Held¹⁷¹, S. Hellman^{148a,148b}, C. Helsens³², R.C.W. Henderson⁷⁵, Y. Heng¹⁷⁶, S. Henkelmann¹⁷¹, A.M. Henriques Correia³², S. Henrot-Versille¹¹⁹, G.H. Herbert¹⁷, H. Herde²⁵, V. Herget¹⁷⁷, Y. Hernández Jiménez^{147c}, H. Herr⁸⁶, G. Herten⁵¹, R. Hertenberger¹⁰², L. Hervas³², T.C. Herwig¹²⁴, G.G. Hesketh⁸¹, N.P. Hessey^{163a}, J.W. Hetherly⁴³, S. Higashino⁶⁹, E. Higón-Rodríguez¹⁷⁰, K. Hildebrand³³, E. Hill¹⁷², J.C. Hill³⁰, K.H. Hiller⁴⁵, S.J. Hillier¹⁹, M. Hils⁴⁷, I. Hinchliffe¹⁶, M. Hirose⁵¹, D. Hirschbuehl¹⁷⁸, B. Hiti⁷⁸, O. Hladik¹²⁹, D.R. Hlaluku^{147c}, X. Hoad⁴⁹, J. Hobbs¹⁵⁰, N. Hod^{163a}, M.C. Hodgkinson¹⁴¹, P. Hodgson¹⁴¹, A. Hoecker³², M.R. Hoefkamp¹⁰⁷, F. Hoenig¹⁰², D. Hohn²³, T.R. Holmes³³, M. Homann⁴⁶, S. Honda¹⁶⁴, T. Honda⁶⁹, T.M. Hong¹²⁷, B.H. Hooberman¹⁶⁹, W.H. Hopkins¹¹⁸, Y. Horii¹⁰⁵, A.J. Horton¹⁴⁴, J.-Y. Hostachy⁵⁸, A. Hostiuc¹⁴⁰, S. Hou¹⁵³, A. Hoummada^{137a}, J. Howarth⁸⁷, J. Hoya⁷⁴, M. Hrabovsky¹¹⁷, J. Hrdinka³², I. Hristova¹⁷, J. Hrivnac¹¹⁹, T. Hryn'ova⁵, A. Hrynevich⁹⁶, P.J. Hsu⁶³, S.-C. Hsu¹⁴⁰, Q. Hu²⁷, S. Hu^{36c}, Y. Huang^{35a}, Z. Hubacek¹³⁰, F. Hubaut⁸⁸, F. Huegging²³, T.B. Huffman¹²², E.W. Hughes³⁸, M. Huhtinen³², R.F.H. Hunter³¹, P. Huo¹⁵⁰, N. Huseynov^{68,b}, J. Huston⁹³, J. Huth⁵⁹, R. Hyneman⁹², G. Iacobucci⁵², G. Iakovidis²⁷, I. Ibragimov¹⁴³, L. Iconomidou-Fayard¹¹⁹, Z. Idrissi^{137e}, P. Iengo³², O. Igonkina^{109,aa}, T. Iizawa¹⁷⁴, Y. Ikegami⁶⁹, M. Ikeno⁶⁹, Y. Ilchenko^{11,ab}, D. Iliadis¹⁵⁶, N. Ilic¹⁴⁵, F. Iltzsche⁴⁷, G. Introzzi^{123a,123b}, P. Ioannou^{9,*}, M. Iodice^{136a}, K. Iordanidou³⁸, V. Ippolito⁵⁹, M.F. Isacson¹⁶⁸, N. Ishijima¹²⁰, M. Ishino¹⁵⁷, M. Ishitsuka¹⁵⁹, C. Issever¹²², S. Istin^{20a}, F. Ito¹⁶⁴, J.M. Iturbe Ponce^{62a}, R. Iuppa^{162a,162b}, H. Iwasaki⁶⁹, J.M. Izen⁴⁴, V. Izzo^{106a}, S. Jabbar³, P. Jackson¹, R.M. Jacobs²³, V. Jain², K.B. Jakobi⁸⁶, K. Jakobs⁵¹, S. Jakobsen⁶⁵, T. Jakoubek¹²⁹, D.O. Jamin¹¹⁶, D.K. Jana⁸², R. Jansky⁵², J. Janssen²³, M. Janus⁵⁷, P.A. Janus^{41a}, G. Jarlskog⁸⁴, N. Javadov^{68,b}, T. Javůrek⁵¹, M. Javurkova⁵¹, F. Jeanneau¹³⁸, L. Jeanty¹⁶,

J. Jejelava ^{54a,ac}, A. Jelinskas ¹⁷³, P. Jenni ^{51,ad}, C. Jeske ¹⁷³, S. Jézéquel ⁵, H. Ji ¹⁷⁶, J. Jia ¹⁵⁰, H. Jiang ⁶⁷, Y. Jiang ^{36a}, Z. Jiang ¹⁴⁵, S. Jiggins ⁸¹, J. Jimenez Pena ¹⁷⁰, S. Jin ^{35b}, A. Jinaru ^{28b}, O. Jinnouchi ¹⁵⁹, H. Jivan ^{147c}, P. Johansson ¹⁴¹, K.A. Johns ⁷, C.A. Johnson ⁶⁴, W.J. Johnson ¹⁴⁰, K. Jon-And ^{148a,148b}, R.W.L. Jones ⁷⁵, S.D. Jones ¹⁵¹, S. Jones ⁷, T.J. Jones ⁷⁷, J. Jongmanns ^{60a}, P.M. Jorge ^{128a,128b}, J. Jovicevic ^{163a}, X. Ju ¹⁷⁶, A. Juste Rozas ^{13,v}, M.K. Köhler ¹⁷⁵, A. Kaczmarska ⁴², M. Kado ¹¹⁹, H. Kagan ¹¹³, M. Kagan ¹⁴⁵, S.J. Kahn ⁸⁸, T. Kaji ¹⁷⁴, E. Kajomovitz ¹⁵⁴, C.W. Kalderon ⁸⁴, A. Kaluza ⁸⁶, S. Kama ⁴³, A. Kamenshchikov ¹³², N. Kanaya ¹⁵⁷, L. Kanjir ⁷⁸, V.A. Kantserov ¹⁰⁰, J. Kanzaki ⁶⁹, B. Kaplan ¹¹², L.S. Kaplan ¹⁷⁶, D. Kar ^{147c}, K. Karakostas ¹⁰, N. Karastathis ¹⁰, M.J. Kareem ^{163b}, E. Karentzos ¹⁰, S.N. Karpov ⁶⁸, Z.M. Karpova ⁶⁸, V. Kartvelishvili ⁷⁵, A.N. Karyukhin ¹³², K. Kasahara ¹⁶⁴, L. Kashif ¹⁷⁶, R.D. Kass ¹¹³, A. Kastanas ¹⁴⁹, Y. Kataoka ¹⁵⁷, C. Kato ¹⁵⁷, A. Katre ⁵², J. Katzy ⁴⁵, K. Kawade ⁷⁰, K. Kawagoe ⁷³, T. Kawamoto ¹⁵⁷, G. Kawamura ⁵⁷, E.F. Kay ⁷⁷, V.F. Kazanin ^{111,c}, R. Keeler ¹⁷², R. Kehoe ⁴³, J.S. Keller ³¹, E. Kellermann ⁸⁴, J.J. Kempster ⁸⁰, J. Kendrick ¹⁹, H. Keoshkerian ¹⁶¹, O. Kepka ¹²⁹, B.P. Kerševan ⁷⁸, S. Kersten ¹⁷⁸, R.A. Keyes ⁹⁰, M. Khader ¹⁶⁹, F. Khalil-zada ¹², A. Khanov ¹¹⁶, A.G. Kharlamov ^{111,c}, T. Kharlamova ^{111,c}, A. Khodinov ¹⁶⁰, T.J. Khoo ⁵², V. Khovanskiy ^{99,*}, E. Khramov ⁶⁸, J. Khubua ^{54b,ae}, S. Kido ⁷⁰, C.R. Kilby ⁸⁰, H.Y. Kim ⁸, S.H. Kim ¹⁶⁴, Y.K. Kim ³³, N. Kimura ¹⁵⁶, O.M. Kind ¹⁷, B.T. King ⁷⁷, D. Kirchmeier ⁴⁷, J. Kirk ¹³³, A.E. Kiryunin ¹⁰³, T. Kishimoto ¹⁵⁷, D. Kisielewska ^{41a}, V. Kitali ⁴⁵, O. Kivernyk ⁵, E. Kladiva ^{146b}, T. Klapdor-Kleingrothaus ⁵¹, M.H. Klein ⁹², M. Klein ⁷⁷, U. Klein ⁷⁷, K. Kleinknecht ⁸⁶, P. Klimek ¹¹⁰, A. Klimentov ²⁷, R. Klingenberg ^{46,*}, T. Klingl ²³, T. Klioutchnikova ³², F.F. Klitzner ¹⁰², E.-E. Kluge ^{60a}, P. Kluit ¹⁰⁹, S. Kluth ¹⁰³, E. Kneringer ⁶⁵, E.B.F.G. Knoops ⁸⁸, A. Knue ¹⁰³, A. Kobayashi ¹⁵⁷, D. Kobayashi ⁷³, T. Kobayashi ¹⁵⁷, M. Kobel ⁴⁷, M. Kocian ¹⁴⁵, P. Kodys ¹³¹, T. Koffas ³¹, E. Koffeman ¹⁰⁹, N.M. Köhler ¹⁰³, T. Koi ¹⁴⁵, M. Kolb ^{60b}, I. Koletsou ⁵, T. Kondo ⁶⁹, N. Kondrashova ^{36c}, K. Köneke ⁵¹, A.C. König ¹⁰⁸, T. Kono ^{69,af}, R. Konoplich ^{112,ag}, N. Konstantinidis ⁸¹, B. Konya ⁸⁴, R. Kopeliansky ⁶⁴, S. Koperny ^{41a}, K. Korcyl ⁴², K. Kordas ¹⁵⁶, A. Korn ⁸¹, I. Korolkov ¹³, E.V. Korolkova ¹⁴¹, O. Kortner ¹⁰³, S. Kortner ¹⁰³, T. Kosek ¹³¹, V.V. Kostyukhin ²³, A. Kotwal ⁴⁸, A. Koulouris ¹⁰, A. Kourkoulis-Charalampidi ^{123a,123b}, C. Kourkoulis ⁹, E. Kourlitis ¹⁴¹, V. Kouskoura ²⁷, A.B. Kowalewska ⁴², R. Kowalewski ¹⁷², T.Z. Kowalski ^{41a}, C. Kozakai ¹⁵⁷, W. Kozanecki ¹³⁸, A.S. Kozhin ¹³², V.A. Kramarenko ¹⁰¹, G. Kramberger ⁷⁸, D. Krasnopevtsev ¹⁰⁰, M.W. Krasny ⁸³, A. Krasznahorkay ³², D. Krauss ¹⁰³, J.A. Kremer ^{41a}, J. Kretzschmar ⁷⁷, K. Kreutzfeldt ⁵⁵, P. Krieger ¹⁶¹, K. Krizka ¹⁶, K. Kroeninger ⁴⁶, H. Kroha ¹⁰³, J. Kroll ¹²⁹, J. Kroll ¹²⁴, J. Kroseberg ²³, J. Krstic ¹⁴, U. Kruchonak ⁶⁸, H. Krüger ²³, N. Krumnack ⁶⁷, M.C. Kruse ⁴⁸, T. Kubota ⁹¹, H. Kucuk ⁸¹, S. Kuday ^{4b}, J.T. Kuechler ¹⁷⁸, S. Kuehn ³², A. Kugel ^{60a}, F. Kuger ¹⁷⁷, T. Kuhl ⁴⁵, V. Kukhtin ⁶⁸, R. Kukla ⁸⁸, Y. Kulchitsky ⁹⁵, S. Kuleshov ^{34b}, Y.P. Kulinich ¹⁶⁹, M. Kuna ¹¹, T. Kunigo ⁷¹, A. Kupco ¹²⁹, T. Kupfer ⁴⁶, O. Kuprash ¹⁵⁵, H. Kurashige ⁷⁰, L.L. Kurchaninov ^{163a}, Y.A. Kurochkin ⁹⁵, M.G. Kurth ^{35a,35d}, E.S. Kuwertz ¹⁷², M. Kuze ¹⁵⁹, J. Kvita ¹¹⁷, T. Kwan ¹⁷², D. Kyriazopoulos ¹⁴¹, A. La Rosa ¹⁰³, J.L. La Rosa Navarro ^{26d}, L. La Rotonda ^{40a,40b}, F. La Ruffa ^{40a,40b}, C. Lacasta ¹⁷⁰, F. Lacava ^{134a,134b}, J. Lacey ⁴⁵, D.P.J. Lack ⁸⁷, H. Lacker ¹⁷, D. Lacour ⁸³, E. Ladygin ⁶⁸, R. Lafaye ⁵, B. Laforge ⁸³, T. Lagouri ¹⁷⁹, S. Lai ⁵⁷, S. Lammers ⁶⁴, W. Lampl ⁷, E. Lançon ²⁷, U. Landgraf ⁵¹, M.P.J. Landon ⁷⁹, M.C. Lanfermann ⁵², V.S. Lang ⁴⁵, J.C. Lange ¹³, R.J. Langenberg ³², A.J. Lankford ¹⁶⁶, F. Lanni ²⁷, K. Lantzscheid ²³, A. Lanza ^{123a}, A. Lapertosa ^{53a,53b}, S. Laplace ⁸³, J.F. Laporte ¹³⁸, T. Lari ^{94a}, F. Lasagni Manghi ^{22a,22b}, M. Lassnig ³², T.S. Lau ^{62a}, P. Laurelli ⁵⁰, W. Lavrijsen ¹⁶, A.T. Law ¹³⁹, P. Laycock ⁷⁷, T. Lazovich ⁵⁹, M. Lazzaroni ^{94a,94b}, B. Le ⁹¹, O. Le Dortz ⁸³, E. Le Guirriec ⁸⁸, E.P. Le Quilleuc ¹³⁸, M. LeBlanc ⁷, T. LeCompte ⁶, F. Ledroit-Guillon ⁵⁸, C.A. Lee ²⁷, G.R. Lee ^{34a}, S.C. Lee ¹⁵³, L. Lee ⁵⁹, B. Lefebvre ⁹⁰, G. Lefebvre ⁸³, M. Lefebvre ¹⁷², F. Legger ¹⁰², C. Leggett ¹⁶, G. Lehmann Miotto ³², X. Lei ⁷, W.A. Leight ⁴⁵, M.A.L. Leite ^{26d}, R. Leitner ¹³¹, D. Lellouch ¹⁷⁵, B. Lemmer ⁵⁷, K.J.C. Leney ⁸¹, T. Lenz ²³, B. Lenzi ³², R. Leone ⁷, S. Leone ^{126a,126b}, C. Leonidopoulos ⁴⁹, G. Lerner ¹⁵¹, C. Leroy ⁹⁷, R. Les ¹⁶¹, A.A.J. Lesage ¹³⁸, C.G. Lester ³⁰, M. Levchenko ¹²⁵, J. Levêque ⁵, D. Levin ⁹², L.J. Levinson ¹⁷⁵, M. Levy ¹⁹, D. Lewis ⁷⁹, B. Li ^{36a,w}, H. Li ¹⁵⁰, L. Li ^{36c}, Q. Li ^{35a,35d}, Q. Li ^{36a}, S. Li ⁴⁸, X. Li ^{36c}, Y. Li ¹⁴³, Z. Liang ^{35a}, B. Liberti ^{135a}, A. Liblong ¹⁶¹, K. Lie ^{62c}, W. Liebig ¹⁵, A. Limosani ¹⁵², C.Y. Lin ³⁰, K. Lin ⁹³, S.C. Lin ¹⁸², T.H. Lin ⁸⁶, R.A. Linck ⁶⁴, B.E. Lindquist ¹⁵⁰, A.E. Lioni ⁵², E. Lipeles ¹²⁴, A. Lipniacka ¹⁵, M. Lisovsky ^{60b}, T.M. Liss ^{169,ah}, A. Lister ¹⁷¹, A.M. Litke ¹³⁹, B. Liu ⁶⁷, H. Liu ⁹², H. Liu ²⁷, J.K.K. Liu ¹²², J. Liu ^{36b}, J.B. Liu ^{36a}, K. Liu ⁸⁸, L. Liu ¹⁶⁹, M. Liu ^{36a}, Y.L. Liu ^{36a}, Y. Liu ^{36a}, M. Livan ^{123a,123b}, A. Lleres ⁵⁸, J. Llorente Merino ^{35a}, S.L. Lloyd ⁷⁹, C.Y. Lo ^{62b}, F. Lo Sterzo ⁴³, E.M. Lobodzinska ⁴⁵, P. Loch ⁷, F.K. Loebinger ⁸⁷, A. Loesle ⁵¹, K.M. Loew ²⁵, T. Lohse ¹⁷, K. Lohwasser ¹⁴¹, M. Lokajicek ¹²⁹, B.A. Long ²⁴,

J.D. Long¹⁶⁹, R.E. Long⁷⁵, L. Longo^{76a,76b}, K.A. Looper¹¹³, J.A. Lopez^{34b}, I. Lopez Paz¹³, A. Lopez Solis⁸³, J. Lorenz¹⁰², N. Lorenzo Martinez⁵, M. Losada²¹, P.J. Lösel¹⁰², X. Lou^{35a}, A. Lounis¹¹⁹, J. Love⁶, P.A. Love⁷⁵, H. Lu^{62a}, N. Lu⁹², Y.J. Lu⁶³, H.J. Lubatti¹⁴⁰, C. Luci^{134a,134b}, A. Lucotte⁵⁸, C. Luedtke⁵¹, F. Luehring⁶⁴, W. Lukas⁶⁵, L. Luminari^{134a}, B. Lund-Jensen¹⁴⁹, M.S. Lutz⁸⁹, P.M. Luzi⁸³, D. Lynn²⁷, R. Lysak¹²⁹, E. Lytken⁸⁴, F. Lyu^{35a}, V. Lyubushkin⁶⁸, H. Ma²⁷, L.L. Ma^{36b}, Y. Ma^{36b}, G. Maccarrone⁵⁰, A. Macchiolo¹⁰³, C.M. Macdonald¹⁴¹, B. Maček⁷⁸, J. Machado Miguens^{124,128b}, D. Madaffari¹⁷⁰, R. Madar³⁷, W.F. Mader⁴⁷, A. Madsen⁴⁵, N. Madysa⁴⁷, J. Maeda⁷⁰, S. Maeland¹⁵, T. Maeno²⁷, A.S. Maevskiy¹⁰¹, V. Magerl⁵¹, C. Maiani¹¹⁹, C. Maidantchik^{26a}, T. Maier¹⁰², A. Maio^{128a,128b,128d}, O. Majersky^{146a}, S. Majewski¹¹⁸, Y. Makida⁶⁹, N. Makovec¹¹⁹, B. Malaescu⁸³, Pa. Malecki⁴², V.P. Maleev¹²⁵, F. Malek⁵⁸, U. Mallik⁶⁶, D. Malon⁶, C. Malone³⁰, S. Maltezos¹⁰, S. Malyukov³², J. Mamuzic¹⁷⁰, G. Mancini⁵⁰, I. Mandić⁷⁸, J. Maneira^{128a,128b}, L. Manhaes de Andrade Filho^{26b}, J. Manjarres Ramos⁴⁷, K.H. Mankinen⁸⁴, A. Mann¹⁰², A. Manousos³², B. Mansoulie¹³⁸, J.D. Mansour^{35a}, R. Mantifel⁹⁰, M. Mantoani⁵⁷, S. Manzoni^{94a,94b}, L. Mapelli³², G. Marceca²⁹, L. March⁵², L. Marchese¹²², G. Marchiori⁸³, M. Marcisovsky¹²⁹, C.A. Marin Tobon³², M. Marjanovic³⁷, D.E. Marley⁹², F. Marroquim^{26a}, S.P. Marsden⁸⁷, Z. Marshall¹⁶, M.U.F. Martensson¹⁶⁸, S. Marti-Garcia¹⁷⁰, C.B. Martin¹¹³, T.A. Martin¹⁷³, V.J. Martin⁴⁹, B. Martin dit Latour¹⁵, M. Martinez^{13,v}, V.I. Martinez Outschoorn¹⁶⁹, S. Martin-Haugh¹³³, V.S. Martoiu^{28b}, A.C. Martyniuk⁸¹, A. Marzin³², L. Masetti⁸⁶, T. Mashimo¹⁵⁷, R. Mashinistov⁹⁸, J. Masik⁸⁷, A.L. Maslennikov^{111,c}, L.H. Mason⁹¹, L. Massa^{135a,135b}, P. Mastrandrea⁵, A. Mastroberardino^{40a,40b}, T. Masubuchi¹⁵⁷, P. Mättig¹⁷⁸, J. Maurer^{28b}, S.J. Maxfield⁷⁷, D.A. Maximov^{111,c}, R. Mazini¹⁵³, I. Maznas¹⁵⁶, S.M. Mazza^{94a,94b}, N.C. Mc Fadden¹⁰⁷, G. Mc Goldrick¹⁶¹, S.P. Mc Kee⁹², A. McCarn⁹², R.L. McCarthy¹⁵⁰, T.G. McCarthy¹⁰³, L.I. McClymont⁸¹, E.F. McDonald⁹¹, J.A. Mcfayden³², G. Mchedlidze⁵⁷, S.J. McMahon¹³³, P.C. McNamara⁹¹, C.J. McNicol¹⁷³, R.A. McPherson^{172,o}, S. Meehan¹⁴⁰, T.J. Megy⁵¹, S. Mehlhase¹⁰², A. Mehta⁷⁷, T. Meideck⁵⁸, K. Meier^{60a}, B. Meirose⁴⁴, D. Melini^{170,ai}, B.R. Mellado Garcia^{147c}, J.D. Mellenthin⁵⁷, M. Melo^{146a}, F. Meloni¹⁸, A. Melzer²³, S.B. Menary⁸⁷, L. Meng⁷⁷, X.T. Meng⁹², A. Mengarelli^{22a,22b}, S. Menke¹⁰³, E. Meoni^{40a,40b}, S. Mergelmeyer¹⁷, C. Merlassino¹⁸, P. Mermod⁵², L. Merola^{106a,106b}, C. Meroni^{94a}, F.S. Merritt³³, A. Messina^{134a,134b}, J. Metcalfe⁶, A.S. Mete¹⁶⁶, C. Meyer¹²⁴, J.-P. Meyer¹³⁸, J. Meyer¹⁰⁹, H. Meyer Zu Theenhausen^{60a}, F. Miano¹⁵¹, R.P. Middleton¹³³, S. Miglioranza^{53a,53b}, L. Mijović⁴⁹, G. Mikenberg¹⁷⁵, M. Mikestikova¹²⁹, M. Mikuž⁷⁸, M. Milesi⁹¹, A. Milic¹⁶¹, D.A. Millar⁷⁹, D.W. Miller³³, C. Mills⁴⁹, A. Milov¹⁷⁵, D.A. Milstead^{148a,148b}, A.A. Minaenko¹³², Y. Minami¹⁵⁷, I.A. Minashvili^{54b}, A.I. Mincer¹¹², B. Mindur^{41a}, M. Mineev⁶⁸, Y. Minegishi¹⁵⁷, Y. Ming¹⁷⁶, L.M. Mir¹³, A. Mirto^{76a,76b}, K.P. Mistry¹²⁴, T. Mitani¹⁷⁴, J. Mitrevski¹⁰², V.A. Mitsou¹⁷⁰, A. Miucci¹⁸, P.S. Miyagawa¹⁴¹, A. Mizukami⁶⁹, J.U. Mjörnmark⁸⁴, T. Mkrtchyan¹⁸⁰, M. Mlynarikova¹³¹, T. Moa^{148a,148b}, K. Mochizuki⁹⁷, P. Mogg⁵¹, S. Mohapatra³⁸, S. Molander^{148a,148b}, R. Moles-Valls²³, M.C. Mondragon⁹³, K. Mönig⁴⁵, J. Monk³⁹, E. Monnier⁸⁸, A. Montalbano¹⁵⁰, J. Montejo Berlingen³², F. Monticelli⁷⁴, S. Monzani^{94a,94b}, R.W. Moore³, N. Morange¹¹⁹, D. Moreno²¹, M. Moreno Llacer³², P. Morettini^{53a}, M. Morgenstern¹⁰⁹, S. Morgenstern³², D. Mori¹⁴⁴, T. Mori¹⁵⁷, M. Morii⁵⁹, M. Morinaga¹⁷⁴, V. Morisbak¹²¹, A.K. Morley³², G. Mornacchi³², J.D. Morris⁷⁹, L. Morvaj¹⁵⁰, P. Moschovakos¹⁰, M. Mosidze^{54b}, H.J. Moss¹⁴¹, J. Moss^{145,aj}, K. Motohashi¹⁵⁹, R. Mount¹⁴⁵, E. Mountricha²⁷, E.J.W. Moyse⁸⁹, S. Muanza⁸⁸, F. Mueller¹⁰³, J. Mueller¹²⁷, R.S.P. Mueller¹⁰², D. Muenstermann⁷⁵, P. Mullen⁵⁶, G.A. Mullier¹⁸, F.J. Munoz Sanchez⁸⁷, W.J. Murray^{173,133}, H. Musheghyan³², M. Muškinja⁷⁸, C. Mwewa^{147a}, A.G. Myagkov^{132,ak}, M. Myska¹³⁰, B.P. Nachman¹⁶, O. Nackenhorst⁵², K. Nagai¹²², R. Nagai^{69,af}, K. Nagano⁶⁹, Y. Nagasaka⁶¹, K. Nagata¹⁶⁴, M. Nagel⁵¹, E. Nagy⁸⁸, A.M. Nairz³², Y. Nakahama¹⁰⁵, K. Nakamura⁶⁹, T. Nakamura¹⁵⁷, I. Nakano¹¹⁴, R.F. Naranjo Garcia⁴⁵, R. Narayan¹¹, D.I. Narrias Villar^{60a}, I. Naryshkin¹²⁵, T. Naumann⁴⁵, G. Navarro²¹, R. Nayyar⁷, H.A. Neal⁹², P.Yu. Nechaeva⁹⁸, T.J. Neep¹³⁸, A. Negri^{123a,123b}, M. Negrini^{22a}, S. Nektarijevic¹⁰⁸, C. Nellist⁵⁷, A. Nelson¹⁶⁶, M.E. Nelson¹²², S. Nemecek¹²⁹, P. Nemethy¹¹², M. Nessi^{32,al}, M.S. Neubauer¹⁶⁹, M. Neumann¹⁷⁸, P.R. Newman¹⁹, T.Y. Ng^{62c}, Y.S. Ng¹⁷, T. Nguyen Manh⁹⁷, R.B. Nickerson¹²², R. Nicolaidou¹³⁸, J. Nielsen¹³⁹, N. Nikiforou¹¹, V. Nikolaenko^{132,ak}, I. Nikolic-Audit⁸³, K. Nikolopoulos¹⁹, P. Nilsson²⁷, Y. Ninomiya⁶⁹, A. Nisati^{134a}, N. Nishu^{36c}, R. Nisius¹⁰³, I. Nitsche⁴⁶, T. Nitta¹⁷⁴, T. Nobe¹⁵⁷, Y. Noguchi⁷¹, M. Nomachi¹²⁰, I. Nomidis³¹, M.A. Nomura²⁷, T. Nooney⁷⁹, M. Nordberg³², N. Norjoharuddeen¹²², O. Novgorodova⁴⁷,

M. Nozaki⁶⁹, L. Nozka¹¹⁷, K. Ntekas¹⁶⁶, E. Nurse⁸¹, F. Nuti⁹¹, K. O'Connor²⁵, D.C. O'Neil¹⁴⁴, A.A. O'Rourke⁴⁵, V. O'Shea⁵⁶, F.G. Oakham^{31,d}, H. Oberlack¹⁰³, T. Obermann²³, J. Ocariz⁸³, A. Ochi⁷⁰, I. Ochoa³⁸, J.P. Ochoa-Ricoux^{34a}, S. Oda⁷³, S. Odaka⁶⁹, A. Oh⁸⁷, S.H. Oh⁴⁸, C.C. Ohm¹⁴⁹, H. Ohman¹⁶⁸, H. Oide^{53a,53b}, H. Okawa¹⁶⁴, Y. Okumura¹⁵⁷, T. Okuyama⁶⁹, A. Olariu^{28b}, L.F. Oleiro Seabra^{128a}, S.A. Olivares Pino^{34a}, D. Oliveira Damazio²⁷, M.J.R. Olsson³³, A. Olszewski⁴², J. Olszowska⁴², A. Onofre^{128a,128e}, K. Onogi¹⁰⁵, P.U.E. Onyisi^{11,ab}, H. Oppen¹²¹, M.J. Oreglia³³, Y. Oren¹⁵⁵, D. Orestano^{136a,136b}, N. Orlando^{62b}, R.S. Orr¹⁶¹, B. Osculati^{53a,53b,*}, R. Ospanov^{36a}, G. Otero y Garzon²⁹, H. Otono⁷³, M. Ouchrif^{137d}, F. Ould-Saada¹²¹, A. Ouraou¹³⁸, K.P. Oussoren¹⁰⁹, Q. Ouyang^{35a}, M. Owen⁵⁶, R.E. Owen¹⁹, V.E. Ozcan^{20a}, N. Ozturk⁸, K. Pachal¹⁴⁴, A. Pacheco Pages¹³, L. Pacheco Rodriguez¹³⁸, C. Padilla Aranda¹³, S. Pagan Griso¹⁶, M. Paganini¹⁷⁹, F. Paige²⁷, G. Palacino⁶⁴, S. Palazzo^{40a,40b}, S. Palestini³², M. Palka^{41b}, D. Pallin³⁷, E. St. Panagiotopoulou¹⁰, I. Panagoulas¹⁰, C.E. Pandini⁵², J.G. Panduro Vazquez⁸⁰, P. Pani³², S. Panitkin²⁷, D. Pantea^{28b}, L. Paolozzi⁵², Th.D. Papadopoulos¹⁰, K. Papageorgiou^{9,s}, A. Paramonov⁶, D. Paredes Hernandez¹⁷⁹, A.J. Parker⁷⁵, M.A. Parker³⁰, K.A. Parker⁴⁵, F. Parodi^{53a,53b}, J.A. Parsons³⁸, U. Parzefall⁵¹, V.R. Pascuzzi¹⁶¹, J.M. Pasner¹³⁹, E. Pasqualucci^{134a}, S. Passaggio^{53a}, Fr. Pastore⁸⁰, S. Patariaia⁸⁶, J.R. Pater⁸⁷, T. Pauly³², B. Pearson¹⁰³, S. Pedraza Lopez¹⁷⁰, R. Pedro^{128a,128b}, S.V. Peleganchuk^{111,c}, O. Penc¹²⁹, C. Peng^{35a,35d}, H. Peng^{36a}, J. Penwell⁶⁴, B.S. Peralva^{26b}, M.M. Perego¹³⁸, D.V. Perepelitsa²⁷, F. Peri¹⁷, L. Perini^{94a,94b}, H. Pernegger³², S. Perrella^{106a,106b}, R. Peschke⁴⁵, V.D. Peshekhonov^{68,*}, K. Peters⁴⁵, R.F.Y. Peters⁸⁷, B.A. Petersen³², T.C. Petersen³⁹, E. Petit⁵⁸, A. Petridis¹, C. Petridou¹⁵⁶, P. Petroff¹¹⁹, E. Petrolo^{134a}, M. Petrov¹²², F. Petrucci^{136a,136b}, N.E. Pettersson⁸⁹, A. Peyaud¹³⁸, R. Pezoa^{34b}, F.H. Phillips⁹³, P.W. Phillips¹³³, G. Piacquadio¹⁵⁰, E. Pianori¹⁷³, A. Picazio⁸⁹, M.A. Pickering¹²², R. Piegaia²⁹, J.E. Pilcher³³, A.D. Pilkington⁸⁷, M. Pinamonti^{135a,135b}, J.L. Pinfold³, H. Pirumov⁴⁵, M. Pitt¹⁷⁵, L. Plazak^{146a}, M.-A. Pleier²⁷, V. Pleskot⁸⁶, E. Plotnikova⁶⁸, D. Pluth⁶⁷, P. Podberezko¹¹¹, R. Poettgen⁸⁴, R. Poggi^{123a,123b}, L. Poggioli¹¹⁹, I. Pogrebnyak⁹³, D. Pohl²³, I. Pokharel⁵⁷, G. Polesello^{123a}, A. Poley⁴⁵, A. Policicchio^{40a,40b}, R. Polifka³², A. Polini^{22a}, C.S. Pollard⁵⁶, V. Polychronakos²⁷, K. Pommès³², D. Ponomarenko¹⁰⁰, L. Pontecorvo^{134a}, G.A. Popeneciu^{28d}, D.M. Portillo Quintero⁸³, S. Pospisil¹³⁰, K. Potamianos⁴⁵, I.N. Potrap⁶⁸, C.J. Potter³⁰, H. Potti¹¹, T. Poulsen⁸⁴, J. Poveda³², M.E. Pozo Astigarraga³², P. Pralavorio⁸⁸, A. Pranko¹⁶, S. Prell⁶⁷, D. Price⁸⁷, M. Primavera^{76a}, S. Prince⁹⁰, N. Proklova¹⁰⁰, K. Prokofiev^{62c}, F. Prokoshin^{34b}, S. Protopopescu²⁷, J. Proudfoot⁶, M. Przybycien^{41a}, A. Puri¹⁶⁹, P. Puzo¹¹⁹, J. Qian⁹², Y. Qin⁸⁷, A. Quadt⁵⁷, M. Queitsch-Maitland⁴⁵, D. Quilty⁵⁶, S. Raddum¹²¹, V. Radeka²⁷, V. Radescu¹²², S.K. Radhakrishnan¹⁵⁰, P. Radloff¹¹⁸, P. Rados⁹¹, F. Ragusa^{94a,94b}, G. Rahal¹⁸¹, J.A. Raine⁸⁷, S. Rajagopalan²⁷, C. Rangel-Smith¹⁶⁸, T. Rashid¹¹⁹, S. Raspopov⁵, M.G. Ratti^{94a,94b}, D.M. Rauch⁴⁵, F. Rauscher¹⁰², S. Rave⁸⁶, I. Ravinovich¹⁷⁵, J.H. Rawling⁸⁷, M. Raymond³², A.L. Read¹²¹, N.P. Readioff⁵⁸, M. Reale^{76a,76b}, D.M. Rebuzzi^{123a,123b}, A. Redelbach¹⁷⁷, G. Redlinger²⁷, R. Reece¹³⁹, R.G. Reed^{147c}, K. Reeves⁴⁴, L. Rehnisch¹⁷, J. Reichert¹²⁴, A. Reiss⁸⁶, C. Rembser³², H. Ren^{35a,35d}, M. Rescigno^{134a}, S. Resconi^{94a}, E.D. Resseguie¹²⁴, S. Rettie¹⁷¹, E. Reynolds¹⁹, O.L. Rezanova^{111,c}, P. Reznicek¹³¹, R. Rezvani⁹⁷, R. Richter¹⁰³, S. Richter⁸¹, E. Richter-Was^{41b}, O. Ricken²³, M. Ridel⁸³, P. Rieck¹⁰³, C.J. Riegel¹⁷⁸, J. Rieger⁵⁷, O. Rifki¹¹⁵, M. Rijssenbeek¹⁵⁰, A. Rimoldi^{123a,123b}, M. Rimoldi¹⁸, L. Rinaldi^{22a}, G. Ripellino¹⁴⁹, B. Ristić³², E. Ritsch³², I. Riu¹³, F. Rizatdinova¹¹⁶, E. Rizvi⁷⁹, C. Rizzi¹³, R.T. Roberts⁸⁷, S.H. Robertson^{90,o}, A. Robichaud-Veronneau⁹⁰, D. Robinson³⁰, J.E.M. Robinson⁴⁵, A. Robson⁵⁶, E. Rocco⁸⁶, C. Roda^{126a,126b}, Y. Rodina^{88,am}, S. Rodriguez Bosca¹⁷⁰, A. Rodriguez Perez¹³, D. Rodriguez Rodriguez¹⁷⁰, S. Roe³², C.S. Rogan⁵⁹, O. Røhne¹²¹, J. Roloff⁵⁹, A. Romaniouk¹⁰⁰, M. Romano^{22a,22b}, S.M. Romano Saez³⁷, E. Romero Adam¹⁷⁰, N. Rompotis⁷⁷, M. Ronzani⁵¹, L. Roos⁸³, S. Rosati^{134a}, K. Rosbach⁵¹, P. Rose¹³⁹, N.-A. Rosien⁵⁷, E. Rossi^{106a,106b}, L.P. Rossi^{53a}, J.H.N. Rosten³⁰, R. Rosten¹⁴⁰, M. Rotaru^{28b}, J. Rothberg¹⁴⁰, D. Rousseau¹¹⁹, A. Rozanov⁸⁸, Y. Rozen¹⁵⁴, X. Ruan^{147c}, F. Rubbo¹⁴⁵, F. Rühr⁵¹, A. Ruiz-Martinez³¹, Z. Rurikova⁵¹, N.A. Rusakovich⁶⁸, H.L. Russell⁹⁰, J.P. Rutherford⁷, N. Ruthmann³², E.M. Rüttinger⁴⁵, Y.F. Ryabov¹²⁵, M. Rybar¹⁶⁹, G. Rybkin¹¹⁹, S. Ryu⁶, A. Ryzhov¹³², G.F. Rzehorz⁵⁷, A.F. Saavedra¹⁵², G. Sabato¹⁰⁹, S. Sacerdoti²⁹, H.F.-W. Sadrozinski¹³⁹, R. Sadykov⁶⁸, F. Safai Tehrani^{134a}, P. Saha¹¹⁰, M. Sahinsoy^{60a}, M. Saimpert⁴⁵, M. Saito¹⁵⁷, T. Saito¹⁵⁷, H. Sakamoto¹⁵⁷, Y. Sakurai¹⁷⁴, G. Salamanna^{136a,136b}, J.E. Salazar Loyola^{34b}, D. Salek¹⁰⁹, P.H. Sales De Bruin¹⁶⁸, D. Salihagic¹⁰³, A. Salnikov¹⁴⁵, J. Salt¹⁷⁰, D. Salvatore^{40a,40b}, F. Salvatore¹⁵¹, A. Salvucci^{62a,62b,62c}, A. Salzburger³²,

D. Sammel⁵¹, D. Sampsonidis¹⁵⁶, D. Sampsonidou¹⁵⁶, J. Sánchez¹⁷⁰, A. Sanchez Pineda^{167a,167c}, H. Sandaker¹²¹, R.L. Sandbach⁷⁹, C.O. Sander⁴⁵, M. Sandhoff¹⁷⁸, C. Sandoval²¹, D.P.C. Sankey¹³³, M. Sannino^{53a,53b}, Y. Sano¹⁰⁵, A. Sansoni⁵⁰, C. Santoni³⁷, H. Santos^{128a}, I. Santoyo Castillo¹⁵¹, A. Sapronov⁶⁸, J.G. Saraiva^{128a,128d}, O. Sasaki⁶⁹, K. Sato¹⁶⁴, E. Sauvan⁵, G. Savage⁸⁰, P. Savard^{161,d}, N. Savic¹⁰³, C. Sawyer¹³³, L. Sawyer^{82,u}, C. Sbarra^{22a}, A. Sbrizzi^{22a,22b}, T. Scanlon⁸¹, D.A. Scannicchio¹⁶⁶, J. Schaarschmidt¹⁴⁰, P. Schacht¹⁰³, B.M. Schachtner¹⁰², D. Schaefer³³, L. Schaefer¹²⁴, J. Schaeffer⁸⁶, S. Schaepe³², S. Schaetzel^{60b}, U. Schäfer⁸⁶, A.C. Schaffer¹¹⁹, D. Schaile¹⁰², R.D. Schamberger¹⁵⁰, V.A. Schegelsky¹²⁵, D. Scheirich¹³¹, F. Schenck¹⁷, M. Schernau¹⁶⁶, C. Schiavi^{53a,53b}, S. Schier¹³⁹, L.K. Schildgen²³, C. Schillo⁵¹, M. Schioppa^{40a,40b}, S. Schlenker³², K.R. Schmidt-Sommerfeld¹⁰³, K. Schmieden³², C. Schmitt⁸⁶, S. Schmitt⁴⁵, S. Schmitz⁸⁶, U. Schnoor⁵¹, L. Schoeffel¹³⁸, A. Schoening^{60b}, B.D. Schoenrock⁹³, E. Schopf²³, M. Schott⁸⁶, J.F.P. Schouwenberg¹⁰⁸, J. Schovancova³², S. Schramm⁵², N. Schuh⁸⁶, A. Schulte⁸⁶, M.J. Schultens²³, H.-C. Schultz-Coulon^{60a}, M. Schumacher⁵¹, B.A. Schumm¹³⁹, Ph. Schune¹³⁸, A. Schwartzman¹⁴⁵, T.A. Schwarz⁹², H. Schweiger⁸⁷, Ph. Schwemling¹³⁸, R. Schwienhorst⁹³, J. Schwindling¹³⁸, A. Sciandra²³, G. Sciolla²⁵, M. Scornajenghi^{40a,40b}, F. Scuri^{126a,126b}, F. Scutti⁹¹, J. Searcy⁹², P. Seema²³, S.C. Seidel¹⁰⁷, A. Seiden¹³⁹, J.M. Seixas^{26a}, G. Sekhniaidze^{106a}, K. Sekhon⁹², S.J. Sekula⁴³, N. Semprini-Cesari^{22a,22b}, S. Senkin³⁷, C. Serfon¹²¹, L. Serin¹¹⁹, L. Serkin^{167a,167b}, M. Sessa^{136a,136b}, R. Seuster¹⁷², H. Severini¹¹⁵, T. Sfiligoi⁷⁸, F. Sforza¹⁶⁵, A. Sfyrla⁵², E. Shabalina⁵⁷, N.W. Shaikh^{148a,148b}, L.Y. Shan^{35a}, R. Shang¹⁶⁹, J.T. Shank²⁴, M. Shapiro¹⁶, P.B. Shatalov⁹⁹, K. Shaw^{167a,167b}, S.M. Shaw⁸⁷, A. Shcherbakova^{148a,148b}, C.Y. Shehu¹⁵¹, Y. Shen¹¹⁵, N. Sherafati³¹, A.D. Sherman²⁴, P. Sherwood⁸¹, L. Shi^{153,an}, S. Shimizu⁷⁰, C.O. Shimmin¹⁷⁹, M. Shimojima¹⁰⁴, I.P.J. Shipsey¹²², S. Shirabe⁷³, M. Shiyakova^{68,ao}, J. Shlomi¹⁷⁵, A. Shmeleva⁹⁸, D. Shoaleh Saadi⁹⁷, M.J. Shochet³³, S. Shojaii^{94a,94b}, D.R. Shope¹¹⁵, S. Shrestha¹¹³, E. Shulga¹⁰⁰, M.A. Shupe⁷, P. Sicho¹²⁹, A.M. Sickles¹⁶⁹, P.E. Sidebo¹⁴⁹, E. Sideras Haddad^{147c}, O. Sidiropoulou¹⁷⁷, A. Sidoti^{22a,22b}, F. Siegert⁴⁷, Dj. Sijacki¹⁴, J. Silva^{128a,128d}, S.B. Silverstein^{148a}, V. Simak¹³⁰, L. Simic⁶⁸, S. Simion¹¹⁹, E. Simioni⁸⁶, B. Simmons⁸¹, M. Simon⁸⁶, P. Sinervo¹⁶¹, N.B. Sinev¹¹⁸, M. Sioli^{22a,22b}, G. Siragusa¹⁷⁷, I. Siral⁹², S.Yu. Sivoklov¹⁰¹, J. Sjölin^{148a,148b}, M.B. Skinner⁷⁵, P. Skubic¹¹⁵, M. Slater¹⁹, T. Slavicek¹³⁰, M. Slawinska⁴², K. Sliwa¹⁶⁵, R. Slovak¹³¹, V. Smakhtin¹⁷⁵, B.H. Smart⁵, J. Smiesko^{146a}, N. Smirnov¹⁰⁰, S.Yu. Smirnov¹⁰⁰, Y. Smirnov¹⁰⁰, L.N. Smirnova^{101,ap}, O. Smirnova⁸⁴, J.W. Smith⁵⁷, M.N.K. Smith³⁸, R.W. Smith³⁸, M. Smizanska⁷⁵, K. Smolek¹³⁰, A.A. Snesarev⁹⁸, I.M. Snyder¹¹⁸, S. Snyder²⁷, R. Sobie^{172,o}, F. Socher⁴⁷, A. Soffer¹⁵⁵, A. Sogaard⁴⁹, D.A. Soh¹⁵³, G. Sokhrannyi⁷⁸, C.A. Solans Sanchez³², M. Solar¹³⁰, E.Yu. Soldatov¹⁰⁰, U. Soldevila¹⁷⁰, A.A. Solodkov¹³², A. Soloshenko⁶⁸, O.V. Solovyanov¹³², V. Solovyev¹²⁵, P. Sommer¹⁴¹, H. Son¹⁶⁵, A. Sopczak¹³⁰, D. Sosa^{60b}, C.L. Sotiropoulou^{126a,126b}, S. Sottocornola^{123a,123b}, R. Soualah^{167a,167c}, A.M. Soukharev^{111,c}, D. South⁴⁵, B.C. Sowden⁸⁰, S. Spagnolo^{76a,76b}, M. Spalla^{126a,126b}, M. Spangenberg¹⁷³, F. Spanò⁸⁰, D. Sperlich¹⁷, F. Spettel¹⁰³, T.M. Spieker^{60a}, R. Spighi^{22a}, G. Spigo³², L.A. Spiller⁹¹, M. Spousta¹³¹, R.D. St. Denis^{56,*}, A. Stabile^{94a}, R. Stamen^{60a}, S. Stamm¹⁷, E. Stanecka⁴², R.W. Stanek⁶, C. Stanescu^{136a}, M.M. Stanitzki⁴⁵, B.S. Stapf¹⁰⁹, S. Stapnes¹²¹, E.A. Starchenko¹³², G.H. Stark³³, J. Stark⁵⁸, S.H. Stark³⁹, P. Staroba¹²⁹, P. Starovoitov^{60a}, S. Stärz³², R. Staszewski⁴², M. Stegler⁴⁵, P. Steinberg²⁷, B. Stelzer¹⁴⁴, H.J. Stelzer³², O. Stelzer-Chilton^{163a}, H. Stenzel⁵⁵, T.J. Stevenson⁷⁹, G.A. Stewart⁵⁶, M.C. Stockton¹¹⁸, M. Stoebe⁹⁰, G. Stoicea^{28b}, P. Stolte⁵⁷, S. Stonjek¹⁰³, A.R. Stradling⁸, A. Straessner⁴⁷, M.E. Stramaglia¹⁸, J. Strandberg¹⁴⁹, S. Strandberg^{148a,148b}, M. Strauss¹¹⁵, P. Strizenec^{146b}, R. Ströhmer¹⁷⁷, D.M. Strom¹¹⁸, R. Stroynowski⁴³, A. Strubig⁴⁹, S.A. Stucci²⁷, B. Stugu¹⁵, N.A. Styles⁴⁵, D. Su¹⁴⁵, J. Su¹²⁷, S. Suchek^{60a}, Y. Sugaya¹²⁰, M. Suk¹³⁰, V.V. Sulin⁹⁸, DMS Sultan^{162a,162b}, S. Sultansoy^{4c}, T. Sumida⁷¹, S. Sun⁵⁹, X. Sun³, K. Suruliz¹⁵¹, C.J.E. Suster¹⁵², M.R. Sutton¹⁵¹, S. Suzuki⁶⁹, M. Svatos¹²⁹, M. Swiatlowski³³, S.P. Swift², I. Sykora^{146a}, T. Sykora¹³¹, D. Ta⁵¹, K. Tackmann⁴⁵, J. Taenzer¹⁵⁵, A. Taffard¹⁶⁶, R. Tafirout^{163a}, E. Tahirovic⁷⁹, N. Taiblum¹⁵⁵, H. Takai²⁷, R. Takashima⁷², E.H. Takasugi¹⁰³, K. Takeda⁷⁰, T. Takeshita¹⁴², Y. Takubo⁶⁹, M. Talby⁸⁸, A.A. Talyshev^{111,c}, J. Tanaka¹⁵⁷, M. Tanaka¹⁵⁹, R. Tanaka¹¹⁹, R. Tanioka⁷⁰, B.B. Tannenwald¹¹³, S. Tapia Araya^{34b}, S. Tapprogge⁸⁶, S. Tarem¹⁵⁴, G.F. Tartarelli^{94a}, P. Tas¹³¹, M. Tasevsky¹²⁹, T. Tashiro⁷¹, E. Tassi^{40a,40b}, A. Tavares Delgado^{128a,128b}, Y. Tayalati^{137e}, A.C. Taylor¹⁰⁷, A.J. Taylor⁴⁹, G.N. Taylor⁹¹, P.T.E. Taylor⁹¹, W. Taylor^{163b}, P. Teixeira-Dias⁸⁰, D. Temple¹⁴⁴, H. Ten Kate³², P.K. Teng¹⁵³, J.J. Teoh¹²⁰, F. Tepel¹⁷⁸, S. Terada⁶⁹, K. Terashi¹⁵⁷, J. Terron⁸⁵, S. Terzo¹³, M. Testa⁵⁰, R.J. Teuscher^{161,o}, S.J. Thais¹⁷⁹, T. Theveniaux-Pelzer⁸⁸, F. Thiele³⁹,

J.P. Thomas¹⁹, J. Thomas-Wilsker⁸⁰, P.D. Thompson¹⁹, A.S. Thompson⁵⁶, L.A. Thomsen¹⁷⁹,
E. Thomson¹²⁴, Y. Tian³⁸, M.J. Tibbetts¹⁶, R.E. Ticse Torres⁵⁷, V.O. Tikhomirov^{98,aa}, Yu.A. Tikhonov^{111,c},
S. Timoshenko¹⁰⁰, P. Tipton¹⁷⁹, S. Tisserant⁸⁸, K. Todome¹⁵⁹, S. Todorova-Nova⁵, S. Todt⁴⁷, J. Tojo⁷³,
S. Tokár^{146a}, K. Tokushuku⁶⁹, E. Tolley¹¹³, L. Tomlinson⁸⁷, M. Tomoto¹⁰⁵, L. Tompkins^{145,ar}, K. Toms¹⁰⁷,
B. Tong⁵⁹, P. Tornambe⁵¹, E. Torrence¹¹⁸, H. Torres⁴⁷, E. Torró Pastor¹⁴⁰, J. Toth^{88,as}, F. Touchard⁸⁸,
D.R. Tovey¹⁴¹, C.J. Treado¹¹², T. Trefzger¹⁷⁷, F. Tresoldi¹⁵¹, A. Tricoli²⁷, I.M. Trigger^{163a},
S. Trincas-Duvoid⁸³, M.F. Tripiana¹³, W. Trischuk¹⁶¹, B. Trocme⁵⁸, A. Trofymov⁴⁵, C. Troncon^{94a},
M. Trovatelli¹⁷², L. Truong^{147b}, M. Trzebinski⁴², A. Trzupek⁴², K.W. Tsang^{62a}, J.C.-L. Tseng¹²²,
P.V. Tsiareshka⁹⁵, N. Tsirintanis⁹, S. Tsiskaridze¹³, V. Tsiskaridze⁵¹, E.G. Tskhadadze^{54a},
I.I. Tsukerman⁹⁹, V. Tsulaia¹⁶, S. Tsuno⁶⁹, D. Tsybychev¹⁵⁰, Y. Tu^{62b}, A. Tudorache^{28b}, V. Tudorache^{28b},
T.T. Tulbure^{28a}, A.N. Tuna⁵⁹, S. Turchikhin⁶⁸, D. Turgeman¹⁷⁵, I. Turk Cakir^{4b,at}, R. Turra^{94a}, P.M. Tuts³⁸,
G. Ucchielli^{22a,22b}, I. Ueda⁶⁹, M. Ughetto^{148a,148b}, F. Ukegawa¹⁶⁴, G. Unal³², A. Undrus²⁷, G. Unel¹⁶⁶,
F.C. Ungaro⁹¹, Y. Unno⁶⁹, K. Uno¹⁵⁷, J. Urban^{146b}, P. Urquijo⁹¹, P. Urrejola⁸⁶, G. Usai⁸, J. Usui⁶⁹,
L. Vacavant⁸⁸, V. Vacek¹³⁰, B. Vachon⁹⁰, K.O.H. Vadla¹²¹, A. Vaidya⁸¹, C. Valderanis¹⁰²,
E. Valdes Santurio^{148a,148b}, M. Valente⁵², S. Valentinetti^{22a,22b}, A. Valero¹⁷⁰, L. Valéry¹³, A. Vallier⁵,
J.A. Valls Ferrer¹⁷⁰, W. Van Den Wollenberg¹⁰⁹, H. van der Graaf¹⁰⁹, P. van Gemmeren⁶,
J. Van Nieuwkoop¹⁴⁴, I. van Vulpen¹⁰⁹, M.C. van Woerden¹⁰⁹, M. Vanadia^{135a,135b}, W. Vandelli³²,
A. Vaniachine¹⁶⁰, P. Vankov¹⁰⁹, G. Vardanyan¹⁸⁰, R. Vari^{134a}, E.W. Varnes⁷, C. Varni^{53a,53b}, T. Varol⁴³,
D. Varouchas¹¹⁹, A. Vartapetian⁸, K.E. Varvell¹⁵², J.G. Vasquez¹⁷⁹, G.A. Vasquez^{34b}, F. Vazeille³⁷,
D. Vazquez Furelos¹³, T. Vazquez Schroeder⁹⁰, J. Veatch⁵⁷, V. Veeraraghavan⁷, L.M. Veloce¹⁶¹,
F. Veloso^{128a,128c}, S. Veneziano^{134a}, A. Ventura^{76a,76b}, M. Venturi¹⁷², N. Venturi³², V. Vercesi^{123a},
M. Verducci^{136a,136b}, W. Verkerke¹⁰⁹, A.T. Vermeulen¹⁰⁹, J.C. Vermeulen¹⁰⁹, M.C. Vetterli^{144,d},
N. Viaux Maira^{34b}, O. Viazlo⁸⁴, I. Vichou^{169,*}, T. Vickey¹⁴¹, O.E. Vickey Boeriu¹⁴¹, G.H.A. Viehhauser¹²²,
S. Viel¹⁶, L. Vigani¹²², M. Villa^{22a,22b}, M. Villaplana Perez^{94a,94b}, E. Vilucchi⁵⁰, M.G. Vincker³¹,
V.B. Vinogradov⁶⁸, A. Vishwakarma⁴⁵, C. Vittori^{22a,22b}, I. Vivarelli¹⁵¹, S. Vlachos¹⁰, M. Vogel¹⁷⁸,
P. Vokac¹³⁰, G. Volpi¹³, H. von der Schmitt¹⁰³, E. von Toerne²³, V. Vorobel¹³¹, K. Vorobev¹⁰⁰,
M. Vos¹⁷⁰, R. Voss³², J.H. Vosseveld⁷⁷, N. Vranjes¹⁴, M. Vranjes Milosavljevic¹⁴, V. Vrba¹³⁰,
M. Vreeswijk¹⁰⁹, R. Vuillermet³², I. Vukotic³³, P. Wagner²³, W. Wagner¹⁷⁸, J. Wagner-Kuhr¹⁰²,
H. Wahlberg⁷⁴, S. Wahrmund⁴⁷, K. Wakamiya⁷⁰, J. Walder⁷⁵, R. Walker¹⁰², W. Walkowiak¹⁴³,
V. Wallangen^{148a,148b}, C. Wang^{35b}, C. Wang^{36b,au}, F. Wang¹⁷⁶, H. Wang¹⁶, H. Wang³, J. Wang⁴⁵,
J. Wang¹⁵², Q. Wang¹¹⁵, R.-J. Wang⁸³, R. Wang⁶, S.M. Wang¹⁵³, T. Wang³⁸, W. Wang^{153,av},
W. Wang^{36a,aw}, Z. Wang^{36c}, C. Wanotayaroj⁴⁵, A. Warburton⁹⁰, C.P. Ward³⁰, D.R. Wardrope⁸¹,
A. Washbrook⁴⁹, P.M. Watkins¹⁹, A.T. Watson¹⁹, M.F. Watson¹⁹, G. Watts¹⁴⁰, S. Watts⁸⁷, B.M. Waugh⁸¹,
A.F. Webb¹¹, S. Webb⁸⁶, M.S. Weber¹⁸, S.M. Weber^{60a}, S.W. Weber¹⁷⁷, S.A. Weber³¹, J.S. Webster⁶,
A.R. Weidberg¹²², B. Weinert⁶⁴, J. Weingarten⁵⁷, M. Weirich⁸⁶, C. Weiser⁵¹, P.S. Wells³², T. Wenaus²⁷,
T. Wengler³², S. Wenig³², N. Wermes²³, M.D. Werner⁶⁷, P. Werner³², M. Wessels^{60a}, T.D. Weston¹⁸,
K. Whalen¹¹⁸, N.L. Whallon¹⁴⁰, A.M. Wharton⁷⁵, A.S. White⁹², A. White⁸, M.J. White¹, R. White^{34b},
D. Whiteson¹⁶⁶, B.W. Whitmore⁷⁵, F.J. Wickens¹³³, W. Wiedenmann¹⁷⁶, M. Wielders¹³³,
C. Wigglesworth³⁹, L.A.M. Wiik-Fuchs⁵¹, A. Wildauer¹⁰³, F. Wilk⁸⁷, H.G. Wilkens³², H.H. Williams¹²⁴,
S. Williams¹⁰⁹, C. Willis⁹³, S. Willocq⁸⁹, J.A. Wilson¹⁹, I. Wingerter-Seez⁵, E. Winkels¹⁵¹,
F. Winklmeier¹¹⁸, O.J. Winston¹⁵¹, B.T. Winter²³, M. Wittgen¹⁴⁵, M. Wobisch^{82,u}, A. Wolf⁸⁶,
T.M.H. Wolf¹⁰⁹, R. Wolff⁸⁸, M.W. Wolter⁴², H. Wolters^{128a,128c}, V.W.S. Wong¹⁷¹, N.L. Woods¹³⁹,
S.D. Worm¹⁹, B.K. Wosiek⁴², J. Wotschack³², K.W. Wozniak⁴², M. Wu³³, S.L. Wu¹⁷⁶, X. Wu⁵², Y. Wu⁹²,
T.R. Wyatt⁸⁷, B.M. Wynne⁴⁹, S. Xella³⁹, Z. Xi⁹², L. Xia^{35c}, D. Xu^{35a}, L. Xu²⁷, T. Xu¹³⁸, W. Xu⁹²,
B. Yabsley¹⁵², S. Yacoob^{147a}, D. Yamaguchi¹⁵⁹, Y. Yamaguchi¹⁵⁹, A. Yamamoto⁶⁹, S. Yamamoto¹⁵⁷,
T. Yamanaka¹⁵⁷, F. Yamane⁷⁰, M. Yamatani¹⁵⁷, T. Yamazaki¹⁵⁷, Y. Yamazaki⁷⁰, Z. Yan²⁴, H. Yang^{36c},
H. Yang¹⁶, Y. Yang¹⁵³, Z. Yang¹⁵, W.-M. Yao¹⁶, Y.C. Yap⁴⁵, Y. Yasu⁶⁹, E. Yatsenko⁵, K.H. Yau Wong²³,
J. Ye⁴³, S. Ye²⁷, I. Yeletskikh⁶⁸, E. Yigitbasi²⁴, E. Yildirim⁸⁶, K. Yorita¹⁷⁴, K. Yoshihara¹²⁴, C. Young¹⁴⁵,
C.J.S. Young³², J. Yu⁸, J. Yu⁶⁷, S.P.Y. Yuen²³, I. Yusuff^{30,ax}, B. Zabinski⁴², G. Zacharis¹⁰, R. Zaidan¹³,
A.M. Zaitsev^{132,ak}, N. Zakharchuk⁴⁵, J. Zalieckas¹⁵, A. Zaman¹⁵⁰, S. Zambito⁵⁹, D. Zanzi⁹¹,
C. Zeitnitz¹⁷⁸, G. Zemaityte¹²², A. Zemla^{41a}, J.C. Zeng¹⁶⁹, Q. Zeng¹⁴⁵, O. Zenin¹³², T. Ženiš^{146a},
D. Zerwas¹¹⁹, D. Zhang^{36b}, D. Zhang⁹², F. Zhang¹⁷⁶, G. Zhang^{36a,aw}, H. Zhang¹¹⁹, J. Zhang⁶, L. Zhang⁵¹,

L. Zhang^{36a}, M. Zhang¹⁶⁹, P. Zhang^{35b}, R. Zhang²³, R. Zhang^{36a,au}, X. Zhang^{36b}, Y. Zhang^{35a,35d}, Z. Zhang¹¹⁹, X. Zhao⁴³, Y. Zhao^{36b,x}, Z. Zhao^{36a}, A. Zhemchugov⁶⁸, B. Zhou⁹², C. Zhou¹⁷⁶, L. Zhou⁴³, M. Zhou^{35a,35d}, M. Zhou¹⁵⁰, N. Zhou^{36c}, Y. Zhou⁷, C.G. Zhu^{36b}, H. Zhu^{35a}, J. Zhu⁹², Y. Zhu^{36a}, X. Zhuang^{35a}, K. Zhukov⁹⁸, A. Zibell¹⁷⁷, D. Zieminska⁶⁴, N.I. Zimine⁶⁸, C. Zimmermann⁸⁶, S. Zimmermann⁵¹, Z. Zinonos¹⁰³, M. Zinser⁸⁶, M. Ziolkowski¹⁴³, L. Živković¹⁴, G. Zobernig¹⁷⁶, A. Zoccoli^{22a,22b}, R. Zou³³, M. zur Nedden¹⁷, L. Zwalinski³²

¹ Department of Physics, University of Adelaide, Adelaide, Australia

² Physics Department, SUNY Albany, Albany NY, United States

³ Department of Physics, University of Alberta, Edmonton AB, Canada

⁴ (a) Department of Physics, Ankara University, Ankara; (b) Istanbul Aydin University, Istanbul; (c) Division of Physics, TOBB University of Economics and Technology, Ankara, Turkey

⁵ LAPP, CNRS/IN2P3 and Université Savoie Mont Blanc, Annecy-le-Vieux, France

⁶ High Energy Physics Division, Argonne National Laboratory, Argonne IL, United States

⁷ Department of Physics, University of Arizona, Tucson AZ, United States

⁸ Department of Physics, The University of Texas at Arlington, Arlington TX, United States

⁹ Physics Department, National and Kapodistrian University of Athens, Athens, Greece

¹⁰ Physics Department, National Technical University of Athens, Zografou, Greece

¹¹ Department of Physics, The University of Texas at Austin, Austin TX, United States

¹² Institute of Physics, Azerbaijan Academy of Sciences, Baku, Azerbaijan

¹³ Institut de Física d'Altes Energies (IFAE), The Barcelona Institute of Science and Technology, Barcelona, Spain

¹⁴ Institute of Physics, University of Belgrade, Belgrade, Serbia

¹⁵ Department for Physics and Technology, University of Bergen, Bergen, Norway

¹⁶ Physics Division, Lawrence Berkeley National Laboratory and University of California, Berkeley CA, United States

¹⁷ Department of Physics, Humboldt University, Berlin, Germany

¹⁸ Albert Einstein Center for Fundamental Physics and Laboratory for High Energy Physics, University of Bern, Bern, Switzerland

¹⁹ School of Physics and Astronomy, University of Birmingham, Birmingham, United Kingdom

²⁰ (a) Department of Physics, Bogazici University, Istanbul; (b) Department of Physics Engineering, Gaziantep University, Gaziantep; (d) Istanbul Bilgi University, Faculty of Engineering and Natural Sciences, Istanbul; (e) Bahcesehir University, Faculty of Engineering and Natural Sciences, Istanbul, Turkey

²¹ Centro de Investigaciones, Universidad Antonio Narino, Bogota, Colombia

²² (a) INFN Sezione di Bologna; (b) Dipartimento di Fisica e Astronomia, Università di Bologna, Bologna, Italy

²³ Physikalisches Institut, University of Bonn, Bonn, Germany

²⁴ Department of Physics, Boston University, Boston MA, United States

²⁵ Department of Physics, Brandeis University, Waltham MA, United States

²⁶ (a) Universidade Federal do Rio De Janeiro COPPE/EE/IF, Rio de Janeiro; (b) Electrical Circuits Department, Federal University of Juiz de Fora (UFJF), Juiz de Fora; (c) Federal University of Sao Joao del Rei (UFSJ), Sao Joao del Rei; (d) Instituto de Fisica, Universidade de Sao Paulo, Sao Paulo, Brazil

²⁷ Physics Department, Brookhaven National Laboratory, Upton NY, United States

²⁸ (a) Transilvania University of Brasov, Brasov; (b) Horia Hulubei National Institute of Physics and Nuclear Engineering, Bucharest; (c) Department of Physics, Alexandru Ioan Cuza University of Iasi, Iasi; (d) National Institute for Research and Development of Isotopic and Molecular Technologies, Physics Department, Cluj Napoca; (e) University Politehnica Bucharest, Bucharest; (f) West University in Timisoara, Timisoara, Romania

²⁹ Departamento de Fisica, Universidad de Buenos Aires, Buenos Aires, Argentina

³⁰ Cavendish Laboratory, University of Cambridge, Cambridge, United Kingdom

³¹ Department of Physics, Carleton University, Ottawa ON, Canada

³² CERN, Geneva, Switzerland

³³ Enrico Fermi Institute, University of Chicago, Chicago IL, United States

³⁴ (a) Departamento de Fisica, Pontificia Universidad Católica de Chile, Santiago; (b) Departamento de Fisica, Universidad Técnica Federico Santa María, Valparaíso, Chile

³⁵ (a) Institute of High Energy Physics, Chinese Academy of Sciences, Beijing; (b) Department of Physics, Nanjing University, Jiangsu; (c) Physics Department, Tsinghua University, Beijing 100084; (d) University of Chinese Academy of Science (UCAS), Beijing, China

³⁶ (a) Department of Modern Physics and State Key Laboratory of Particle Detection and Electronics, University of Science and Technology of China, Anhui; (b) School of Physics, Shandong University, Shandong; (c) Department of Physics and Astronomy, Key Laboratory for Particle Physics, Astrophysics and Cosmology, Ministry of Education; Shanghai Key Laboratory for Particle Physics and Cosmology, Shanghai Jiao Tong University, Tsung-Dao Lee Institute, China

³⁷ Université Clermont Auvergne, CNRS/IN2P3, LPC, Clermont-Ferrand, France

³⁸ Nevis Laboratory, Columbia University, Irvington NY, United States

³⁹ Niels Bohr Institute, University of Copenhagen, Copenhagen, Denmark

⁴⁰ (a) INFN Gruppo Collegato di Cosenza, Laboratori Nazionali di Frascati; (b) Dipartimento di Fisica, Università della Calabria, Rende, Italy

⁴¹ (a) AGH University of Science and Technology, Faculty of Physics and Applied Computer Science, Krakow; (b) Marian Smoluchowski Institute of Physics, Jagiellonian University, Krakow, Poland

⁴² Institute of Nuclear Physics Polish Academy of Sciences, Krakow, Poland

⁴³ Physics Department, Southern Methodist University, Dallas TX, United States

⁴⁴ Physics Department, University of Texas at Dallas, Richardson TX, United States

⁴⁵ DESY, Hamburg and Zeuthen, Germany

⁴⁶ Lehrstuhl für Experimentelle Physik IV, Technische Universität Dortmund, Dortmund, Germany

⁴⁷ Institut für Kern- und Teilchenphysik, Technische Universität Dresden, Dresden, Germany

⁴⁸ Department of Physics, Duke University, Durham NC, United States

⁴⁹ SUPA – School of Physics and Astronomy, University of Edinburgh, Edinburgh, United Kingdom

⁵⁰ INFN e Laboratori Nazionali di Frascati, Frascati, Italy

⁵¹ Fakultät für Mathematik und Physik, Albert-Ludwigs-Universität, Freiburg, Germany

⁵² Département de Physique Nucléaire et Corpusculaire, Université de Genève, Geneva, Switzerland

⁵³ (a) INFN Sezione di Genova; (b) Dipartimento di Fisica, Università di Genova, Genova, Italy

⁵⁴ (a) E. Andronikashvili Institute of Physics, Iv. Javakishvili Tbilisi State University, Tbilisi; (b) High Energy Physics Institute, Tbilisi State University, Tbilisi, Georgia

⁵⁵ II Physikalisches Institut, Justus-Liebig-Universität Giessen, Giessen, Germany

⁵⁶ SUPA – School of Physics and Astronomy, University of Glasgow, Glasgow, United Kingdom

⁵⁷ II Physikalisches Institut, Georg-August-Universität, Göttingen, Germany

⁵⁸ Laboratoire de Physique Subatomique et de Cosmologie, Université Grenoble-Alpes, CNRS/IN2P3, Grenoble, France

⁵⁹ Laboratory for Particle Physics and Cosmology, Harvard University, Cambridge MA, United States

⁶⁰ (a) Kirchhoff-Institut für Physik, Ruprecht-Karls-Universität Heidelberg, Heidelberg; (b) Physikalisches Institut, Ruprecht-Karls-Universität Heidelberg, Heidelberg, Germany

⁶¹ Faculty of Applied Information Science, Hiroshima Institute of Technology, Hiroshima, Japan

- ⁶² (a) Department of Physics, The Chinese University of Hong Kong, Shatin, N.T., Hong Kong; (b) Department of Physics, The University of Hong Kong, Hong Kong; (c) Department of Physics and Institute for Advanced Study, The Hong Kong University of Science and Technology, Clear Water Bay, Kowloon, Hong Kong, China
- ⁶³ Department of Physics, National Tsing Hua University, Taiwan, Taiwan
- ⁶⁴ Department of Physics, Indiana University, Bloomington IN, United States
- ⁶⁵ Institut für Astro- und Teilchenphysik, Leopold-Franzens-Universität, Innsbruck, Austria
- ⁶⁶ University of Iowa, Iowa City IA, United States
- ⁶⁷ Department of Physics and Astronomy, Iowa State University, Ames IA, United States
- ⁶⁸ Joint Institute for Nuclear Research, JINR Dubna, Dubna, Russia
- ⁶⁹ KEK, High Energy Accelerator Research Organization, Tsukuba, Japan
- ⁷⁰ Graduate School of Science, Kobe University, Kobe, Japan
- ⁷¹ Faculty of Science, Kyoto University, Kyoto, Japan
- ⁷² Kyoto University of Education, Kyoto, Japan
- ⁷³ Research Center for Advanced Particle Physics and Department of Physics, Kyushu University, Fukuoka, Japan
- ⁷⁴ Instituto de Física La Plata, Universidad Nacional de La Plata and CONICET, La Plata, Argentina
- ⁷⁵ Physics Department, Lancaster University, Lancaster, United Kingdom
- ⁷⁶ (a) INFN Sezione di Lecce; (b) Dipartimento di Matematica e Fisica, Università del Salento, Lecce, Italy
- ⁷⁷ Oliver Lodge Laboratory, University of Liverpool, Liverpool, United Kingdom
- ⁷⁸ Department of Experimental Particle Physics, Jožef Stefan Institute and Department of Physics, University of Ljubljana, Ljubljana, Slovenia
- ⁷⁹ School of Physics and Astronomy, Queen Mary University of London, London, United Kingdom
- ⁸⁰ Department of Physics, Royal Holloway University of London, Surrey, United Kingdom
- ⁸¹ Department of Physics and Astronomy, University College London, London, United Kingdom
- ⁸² Louisiana Tech University, Ruston LA, United States
- ⁸³ Laboratoire de Physique Nucléaire et de Hautes Energies, UPMC and Université Paris-Diderot and CNRS/IN2P3, Paris, France
- ⁸⁴ Fysiska institutionen, Lunds universitet, Lund, Sweden
- ⁸⁵ Departamento de Física Teórica C-15, Universidad Autónoma de Madrid, Madrid, Spain
- ⁸⁶ Institut für Physik, Universität Mainz, Mainz, Germany
- ⁸⁷ School of Physics and Astronomy, University of Manchester, Manchester, United Kingdom
- ⁸⁸ CPPM, Aix-Marseille Université and CNRS/IN2P3, Marseille, France
- ⁸⁹ Department of Physics, University of Massachusetts, Amherst MA, United States
- ⁹⁰ Department of Physics, McGill University, Montreal QC, Canada
- ⁹¹ School of Physics, University of Melbourne, Victoria, Australia
- ⁹² Department of Physics, The University of Michigan, Ann Arbor MI, United States
- ⁹³ Department of Physics and Astronomy, Michigan State University, East Lansing MI, United States
- ⁹⁴ (a) INFN Sezione di Milano; (b) Dipartimento di Fisica, Università di Milano, Milano, Italy
- ⁹⁵ B.I. Stepanov Institute of Physics, National Academy of Sciences of Belarus, Minsk, Belarus
- ⁹⁶ Research Institute for Nuclear Problems of Byelorussian State University, Minsk, Belarus
- ⁹⁷ Group of Particle Physics, University of Montreal, Montreal QC, Canada
- ⁹⁸ P.N. Lebedev Physical Institute of the Russian Academy of Sciences, Moscow, Russia
- ⁹⁹ Institute for Theoretical and Experimental Physics (ITEP), Moscow, Russia
- ¹⁰⁰ National Research Nuclear University MEPhI, Moscow, Russia
- ¹⁰¹ D.V. Skobeltsyn Institute of Nuclear Physics, M.V. Lomonosov Moscow State University, Moscow, Russia
- ¹⁰² Fakultät für Physik, Ludwig-Maximilians-Universität München, München, Germany
- ¹⁰³ Max-Planck-Institut für Physik (Werner-Heisenberg-Institut), München, Germany
- ¹⁰⁴ Nagasaki Institute of Applied Science, Nagasaki, Japan
- ¹⁰⁵ Graduate School of Science and Kobayashi-Maskawa Institute, Nagoya University, Nagoya, Japan
- ¹⁰⁶ (a) INFN Sezione di Napoli; (b) Dipartimento di Fisica, Università di Napoli, Napoli, Italy
- ¹⁰⁷ Department of Physics and Astronomy, University of New Mexico, Albuquerque NM, United States
- ¹⁰⁸ Institute for Mathematics, Astrophysics and Particle Physics, Radboud University Nijmegen/Nikhef, Nijmegen, Netherlands
- ¹⁰⁹ Nikhef National Institute for Subatomic Physics and University of Amsterdam, Amsterdam, Netherlands
- ¹¹⁰ Department of Physics, Northern Illinois University, DeKalb IL, United States
- ¹¹¹ Budker Institute of Nuclear Physics, SB RAS, Novosibirsk, Russia
- ¹¹² Department of Physics, New York University, New York NY, United States
- ¹¹³ Ohio State University, Columbus OH, United States
- ¹¹⁴ Faculty of Science, Okayama University, Okayama, Japan
- ¹¹⁵ Homer L. Dodge Department of Physics and Astronomy, University of Oklahoma, Norman OK, United States
- ¹¹⁶ Department of Physics, Oklahoma State University, Stillwater OK, United States
- ¹¹⁷ Palacký University, RCPTM, Olomouc, Czech Republic
- ¹¹⁸ Center for High Energy Physics, University of Oregon, Eugene OR, United States
- ¹¹⁹ LAL, Univ. Paris-Sud, CNRS/IN2P3, Université Paris-Saclay, Orsay, France
- ¹²⁰ Graduate School of Science, Osaka University, Osaka, Japan
- ¹²¹ Department of Physics, University of Oslo, Oslo, Norway
- ¹²² Department of Physics, Oxford University, Oxford, United Kingdom
- ¹²³ (a) INFN Sezione di Pavia; (b) Dipartimento di Fisica, Università di Pavia, Pavia, Italy
- ¹²⁴ Department of Physics, University of Pennsylvania, Philadelphia PA, United States
- ¹²⁵ National Research Centre "Kurchatov Institute", B.P. Konstantinov Petersburg Nuclear Physics Institute, St. Petersburg, Russia
- ¹²⁶ (a) INFN Sezione di Pisa; (b) Dipartimento di Fisica E. Fermi, Università di Pisa, Pisa, Italy
- ¹²⁷ Department of Physics and Astronomy, University of Pittsburgh, Pittsburgh PA, United States
- ¹²⁸ (a) Laboratório de Instrumentação e Física Experimental de Partículas – LIP, Lisboa; (b) Faculdade de Ciências, Universidade de Lisboa, Lisboa; (c) Department of Physics, University of Coimbra, Coimbra; (d) Centro de Física Nuclear da Universidade de Lisboa, Lisboa; (e) Departamento de Física, Universidade do Minho, Braga; (f) Departamento de Física Teórica y del Cosmos, Universidad de Granada, Granada; (g) Dep Física and CEFITEC of Faculdade de Ciências e Tecnologia, Universidade Nova de Lisboa, Caparica, Portugal
- ¹²⁹ Institute of Physics, Academy of Sciences of the Czech Republic, Praha, Czech Republic
- ¹³⁰ Czech Technical University in Prague, Praha, Czech Republic
- ¹³¹ Charles University, Faculty of Mathematics and Physics, Prague, Czech Republic
- ¹³² State Research Center Institute for High Energy Physics (Protvino), NRC KI, Russia
- ¹³³ Particle Physics Department, Rutherford Appleton Laboratory, Didcot, United Kingdom
- ¹³⁴ (a) INFN Sezione di Roma; (b) Dipartimento di Fisica, Sapienza Università di Roma, Roma, Italy
- ¹³⁵ (a) INFN Sezione di Roma Tor Vergata; (b) Dipartimento di Fisica, Università di Roma Tor Vergata, Roma, Italy
- ¹³⁶ (a) INFN Sezione di Roma Tre; (b) Dipartimento di Matematica e Fisica, Università Roma Tre, Roma, Italy

- ¹³⁷ ^(a) *Faculté des Sciences Ain Chock, Réseau Universitaire de Physique des Hautes Energies – Université Hassan II, Casablanca;* ^(b) *Centre National de l'Energie des Sciences Techniques Nucleaires, Rabat;* ^(c) *Faculté des Sciences Semlalia, Université Cadi Ayyad, LPHEA-Marrakech;* ^(d) *Faculté des Sciences, Université Mohamed Premier and LPTPM, Oujda;* ^(e) *Faculté des sciences, Université Mohammed V, Rabat, Morocco*
- ¹³⁸ *DSM/IRFU (Institut de Recherches sur les Lois Fondamentales de l'Univers), CEA Saclay (Commissariat à l'Energie Atomique et aux Energies Alternatives), Gif-sur-Yvette, France*
- ¹³⁹ *Santa Cruz Institute for Particle Physics, University of California Santa Cruz, Santa Cruz CA, United States*
- ¹⁴⁰ *Department of Physics, University of Washington, Seattle WA, United States*
- ¹⁴¹ *Department of Physics and Astronomy, University of Sheffield, Sheffield, United Kingdom*
- ¹⁴² *Department of Physics, Shinshu University, Nagano, Japan*
- ¹⁴³ *Department Physik, Universität Siegen, Siegen, Germany*
- ¹⁴⁴ *Department of Physics, Simon Fraser University, Burnaby BC, Canada*
- ¹⁴⁵ *SLAC National Accelerator Laboratory, Stanford CA, United States*
- ¹⁴⁶ ^(a) *Faculty of Mathematics, Physics & Informatics, Comenius University, Bratislava;* ^(b) *Department of Subnuclear Physics, Institute of Experimental Physics of the Slovak Academy of Sciences, Kosice, Slovak Republic*
- ¹⁴⁷ ^(a) *Department of Physics, University of Cape Town, Cape Town;* ^(b) *Department of Physics, University of Johannesburg, Johannesburg;* ^(c) *School of Physics, University of the Witwatersrand, Johannesburg, South Africa*
- ¹⁴⁸ ^(a) *Department of Physics, Stockholm University;* ^(b) *The Oskar Klein Centre, Stockholm, Sweden*
- ¹⁴⁹ *Physics Department, Royal Institute of Technology, Stockholm, Sweden*
- ¹⁵⁰ *Departments of Physics & Astronomy and Chemistry, Stony Brook University, Stony Brook NY, United States*
- ¹⁵¹ *Department of Physics and Astronomy, University of Sussex, Brighton, United Kingdom*
- ¹⁵² *School of Physics, University of Sydney, Sydney, Australia*
- ¹⁵³ *Institute of Physics, Academia Sinica, Taipei, Taiwan*
- ¹⁵⁴ *Department of Physics, Technion: Israel Institute of Technology, Haifa, Israel*
- ¹⁵⁵ *Raymond and Beverly Sackler School of Physics and Astronomy, Tel Aviv University, Tel Aviv, Israel*
- ¹⁵⁶ *Department of Physics, Aristotle University of Thessaloniki, Thessaloniki, Greece*
- ¹⁵⁷ *International Center for Elementary Particle Physics and Department of Physics, The University of Tokyo, Tokyo, Japan*
- ¹⁵⁸ *Graduate School of Science and Technology, Tokyo Metropolitan University, Tokyo, Japan*
- ¹⁵⁹ *Department of Physics, Tokyo Institute of Technology, Tokyo, Japan*
- ¹⁶⁰ *Tomsk State University, Tomsk, Russia*
- ¹⁶¹ *Department of Physics, University of Toronto, Toronto ON, Canada*
- ¹⁶² ^(a) *INFN-TIFPA;* ^(b) *University of Trento, Trento, Italy*
- ¹⁶³ ^(a) *TRIUMF, Vancouver BC;* ^(b) *Department of Physics and Astronomy, York University, Toronto ON, Canada*
- ¹⁶⁴ *Faculty of Pure and Applied Sciences, and Center for Integrated Research in Fundamental Science and Engineering, University of Tsukuba, Tsukuba, Japan*
- ¹⁶⁵ *Department of Physics and Astronomy, Tufts University, Medford MA, United States*
- ¹⁶⁶ *Department of Physics and Astronomy, University of California Irvine, Irvine CA, United States*
- ¹⁶⁷ ^(a) *INFN Gruppo Collegato di Udine, Sezione di Trieste, Udine;* ^(b) *ICTP, Trieste;* ^(c) *Dipartimento di Chimica, Fisica e Ambiente, Università di Udine, Udine, Italy*
- ¹⁶⁸ *Department of Physics and Astronomy, University of Uppsala, Uppsala, Sweden*
- ¹⁶⁹ *Department of Physics, University of Illinois, Urbana IL, United States*
- ¹⁷⁰ *Instituto de Física Corpuscular (IFIC), Centro Mixto Universidad de Valencia – CSIC, Spain*
- ¹⁷¹ *Department of Physics, University of British Columbia, Vancouver BC, Canada*
- ¹⁷² *Department of Physics and Astronomy, University of Victoria, Victoria BC, Canada*
- ¹⁷³ *Department of Physics, University of Warwick, Coventry, United Kingdom*
- ¹⁷⁴ *Waseda University, Tokyo, Japan*
- ¹⁷⁵ *Department of Particle Physics, The Weizmann Institute of Science, Rehovot, Israel*
- ¹⁷⁶ *Department of Physics, University of Wisconsin, Madison WI, United States*
- ¹⁷⁷ *Fakultät für Physik und Astronomie, Julius-Maximilians-Universität, Würzburg, Germany*
- ¹⁷⁸ *Fakultät für Mathematik und Naturwissenschaften, Fachgruppe Physik, Bergische Universität Wuppertal, Wuppertal, Germany*
- ¹⁷⁹ *Department of Physics, Yale University, New Haven CT, United States*
- ¹⁸⁰ *Yerevan Physics Institute, Yerevan, Armenia*
- ¹⁸¹ *Centre de Calcul de l'Institut National de Physique Nucléaire et de Physique des Particules (IN2P3), Villeurbanne, France*
- ¹⁸² *Academia Sinica Grid Computing, Institute of Physics, Academia Sinica, Taipei, Taiwan*

^a Also at Department of Physics, King's College London, London, United Kingdom.

^b Also at Institute of Physics, Azerbaijan Academy of Sciences, Baku, Azerbaijan.

^c Also at Novosibirsk State University, Novosibirsk, Russia.

^d Also at TRIUMF, Vancouver BC, Canada.

^e Also at Department of Physics & Astronomy, University of Louisville, Louisville, KY, United States of America.

^f Also at Physics Department, An-Najah National University, Nablus, Palestine.

^g Also at Department of Physics, California State University, Fresno CA, United States of America.

^h Also at Department of Physics, University of Fribourg, Fribourg, Switzerland.

ⁱ Also at II Physikalisches Institut, Georg-August-Universität, Göttingen, Germany.

^j Also at Departament de Física de la Universitat Autònoma de Barcelona, Barcelona, Spain.

^k Also at Departamento de Física e Astronomia, Faculdade de Ciências, Universidade do Porto, Portugal.

^l Also at Tomsk State University, Tomsk, and Moscow Institute of Physics and Technology State University, Dolgoprudny, Russia.

^m Also at The Collaborative Innovation Center of Quantum Matter (CICQM), Beijing, China.

ⁿ Also at Università di Napoli Parthenope, Napoli, Italy.

^o Also at Institute of Particle Physics (IPP), Canada.

^p Also at Horia Hulubei National Institute of Physics and Nuclear Engineering, Bucharest, Romania.

^q Also at Department of Physics, St. Petersburg State Polytechnical University, St. Petersburg, Russia.

^r Also at Borough of Manhattan Community College, City University of New York, New York City, United States of America.

^s Also at Department of Financial and Management Engineering, University of the Aegean, Chios, Greece.

^t Also at Centre for High Performance Computing, CSIR Campus, Rosebank, Cape Town, South Africa.

^u Also at Louisiana Tech University, Ruston LA, United States of America.

^v Also at Institutio Catalana de Recerca i Estudis Avançats, ICREA, Barcelona, Spain.

^w Also at Department of Physics, The University of Michigan, Ann Arbor MI, United States of America.

^x Also at LAL, Univ. Paris-Sud, CNRS/IN2P3, Université Paris-Saclay, Orsay, France.

^y Also at Graduate School of Science, Osaka University, Osaka, Japan.

^z Also at Fakultät für Mathematik und Physik, Albert-Ludwigs-Universität, Freiburg, Germany.

- ^{aa} Also at Institute for Mathematics, Astrophysics and Particle Physics, Radboud University Nijmegen/Nikhef, Nijmegen, Netherlands.
- ^{ab} Also at Department of Physics, The University of Texas at Austin, Austin TX, United States of America.
- ^{ac} Also at Institute of Theoretical Physics, Ilia State University, Tbilisi, Georgia.
- ^{ad} Also at CERN, Geneva, Switzerland.
- ^{ae} Also at Georgian Technical University (GTU), Tbilisi, Georgia.
- ^{af} Also at Ochadai Academic Production, Ochanomizu University, Tokyo, Japan.
- ^{ag} Also at Manhattan College, New York NY, United States of America.
- ^{ah} Also at The City College of New York, New York NY, United States of America.
- ^{ai} Also at Departamento de Física Teórica y del Cosmos, Universidad de Granada, Granada, Spain.
- ^{aj} Also at Department of Physics, California State University, Sacramento CA, United States of America.
- ^{ak} Also at Moscow Institute of Physics and Technology State University, Dolgoprudny, Russia.
- ^{al} Also at Departement de Physique Nucleaire et Corpusculaire, Université de Genève, Geneva, Switzerland.
- ^{am} Also at Institut de Física d'Altes Energies (IFAE), The Barcelona Institute of Science and Technology, Barcelona, Spain.
- ^{an} Also at School of Physics, Sun Yat-sen University, Guangzhou, China.
- ^{ao} Also at Institute for Nuclear Research and Nuclear Energy (INRNE) of the Bulgarian Academy of Sciences, Sofia, Bulgaria.
- ^{ap} Also at Faculty of Physics, M.V.Lomonosov Moscow State University, Moscow, Russia.
- ^{aq} Also at National Research Nuclear University MEPhI, Moscow, Russia.
- ^{ar} Also at Department of Physics, Stanford University, Stanford CA, United States of America.
- ^{as} Also at Institute for Particle and Nuclear Physics, Wigner Research Centre for Physics, Budapest, Hungary.
- ^{at} Also at Giresun University, Faculty of Engineering, Turkey.
- ^{au} Also at CPPM, Aix-Marseille Université and CNRS/IN2P3, Marseille, France.
- ^{av} Also at Department of Physics, Nanjing University, Jiangsu, China.
- ^{aw} Also at Institute of Physics, Academia Sinica, Taipei, Taiwan.
- ^{ax} Also at University of Malaya, Department of Physics, Kuala Lumpur, Malaysia.
- * Deceased.